Center for Air Environment Studies
The Pennsylvania State University

CYCLED OPERATION OF WATER VAPOR ELECTROLYSIS CELL

Annual Report for the period

January 1, 1969 to December 31, 1969

for

National Aeronautics and Space Administration

Grant # NGR-39-009-123

CAES Publication No. 159-70

CAES

THE CENTER FOR AIR ENVIRONMENT STUDIES

The Center for Air Environment Studies at The Pennsylvania State University was established in 1963 to coordinate research and instruction concerning the interaction of man and his air environment. A unit of the interdisciplinary Institute for Science and Engineering, the Center has a staff with backgrounds in many of the physical, biological, social, and allied sciences.

A broad, flexible research program, dependent on faculty and student interest, is maintained by the Center. Some of the current research topics are:

The operation of an air pollution information service utilizing computers and other mechanized systems for the collection, retrieval, and dissemination of air environment literature. "Air Pollution Titles" and "Index to Air Pollution Research," information retrieval periodicals, are produced using computers. (See inside back cover.)

Effects of air pollutants on trees, food, and fiber crops, predisposition to attack by other pathogens, and economic loss through damage to plants.

Studies of small particle behavior.

Development of high accuracy, low cost mobile analysis equipment for routine sampling of ambient air.

Biological effects of air pollutants on animals and natural ecologies.

Studies of basic combustion processes leading to lower contaminant emissions.

A survey of community attitudes toward air pollution.

The description and analysis of the political, legal, and administrative systems for air pollution control through studies in Pennsylvania, New York, and the Delaware Valley.

Study of plume rise and dispersion with analysis of contaminant concentration in the plume.

Development of rapid response, specialized instrumentation for the quantitative measurement of contaminant concentration.

Special studies of gaseous and particulate control devices.

Controlled atmosphere air quality studies for a life-support system.

Fundamental research on the chemistry of airborne contaminants.

Basic facilities and services are maintained and provided by the Center. In addition, through the direct participation of all University Departments, departmental laboratories and facilities are utilized whenever possible. Collectively, these provide an extensive resource for research at The Pennsylvania State University.

The Center has also developed a unique set of educational programs supported by grants from the National Air Pollution Control Administration. In the Graduate Study Program, students conduct thesis work on an air pollution problem in their major field and take a minor course sequence in air pollution topics. In cooperation with the Graduate School and the academic departments, the Center manages the program and organizes the course sequence.

Potential air pollution administrators are prepared in the Introduction to Air Pollution and Control Administration Program, which involves one term of full-time work on campus. This program is offered in the Summer for graduate students

continued on inside back cover

ANNUAL REPORT

on

CYCLED OPERATION OF WATER VAPOR ELECTROLYSIS CELL

to

NATIONAL AERONAUTICS AND SPACE ADMINISTRATION

March 1, 1970

Grant No. NGR 39-009-123

Report Period: January 1, 1969 to December 31, 1969

by

A. J. Engel and A. M. Bloom

Center for Air Environment Studies
The Pennsylvania State University
University Park, Pennsylvania 16802

CAES Publication Number 159-70

TABLE OF CONTENTS

LIST OF FIGURES

Annual Progress Report on

CYCLED OPERATION OF WATER VAPOR ELECTROLYSIS CELL

January 1, 1969 through December 31, 1969

INTRODUCTION

Research on "Cycled Operation of Water Vapor Electrolysis Cell" was carried out under Grant No. NGR 39-009-123 between the National Aeronautics and Space Administration and the Pennsylvania State University and administered through the Center for Air Environment Studies.

The purpose of the study was to investigate the effect of cyclic operation on a water vapor electrolysis cell and the development of a rigorous mathematical model for predicting cell operation under critical conditions.

SUMMARY

A rigorous mathematical model representing the heat, mass, and momentum relationships was developed for digital computation. However, the modelling process revealed a number of gaps in the data previously obtained for the cell. Therefore, it was decided that before any further cycling work would be carried out, these gaps had to be filled.

Experimental studies to determine the equilibrium conditions that exist between the gel matrix and water vapor as a function of acid concentration in the matrix were conducted satisfactorily. Also, the electrical conductance of the matrix was studied for varying silica concentrations.

Finally, the cell hardware components for the cyclic operation studies were built and/or assembled and are now operational.

MATHEMATIC MODEL

WATER VAPOR ELECTROLYSIS CELL

Introduction

Interest in the development of a workable math model of the water vapor electrolysis cell is long-standing. The first such model was developed by Clifford (2) in 1965, and the second by Engel (7, 8) in 1967-8. Both models saw the cell as merely the air flow channel, with the matrix symbolized by a mass sink and a heat source at one wall of the channel. The limited knowledge of the physical-chemical and electrochemical properties of the cell matrix precluded a more realistic model. Both models assumed the situation to be flow of an incompressible fluid through a slit with mass and heat transfer at the "matrix" wall calculated from experimentally determined cell power consumption and assumed constant along the length of the flow channel. Given experimentally determined inlet and exit temperatures and relative humidities, and assumed velocity profiles, available closed-form solutions to the pertinent transport equations were utilized to calculate temperature and concentration profiles for the models. Neither is a true model of the cell, but rather a solution of a set of steady state equations. Their utility is in making first order approximations of the temperature of the matrix, a difficult quantity to measure.

At the beginning of the present work, no more information was available than was available to the two previous workers. The model developed, therefore, also viewed the water vapor electrolysis cell as an air flow channel, the cell matrix being a boundary condition.

Again, average heat and mass transfer at the boundary were calculated from experimental power data.

The model was, however, to be an order of magnitude closer to describing the physical situation and to be closer to a math model of the cell. The air was to be viewed as a compressible fluid and no velocity profile was to be imposed. The model was to predict velocity, temperature, and concentration profiles, as well as the properties of the air stream leaving the cell, given inlet air properties and experimental cell voltage versus current data.

There exists no closed-form solution to the transport equations describing the above situation. Algebraic analysis of finite increments of the flow channel yielded numerical approximations of the pertinent partial differential equations. Then followed development of an algorithm capable of solving the resulting system of simultaneous non-linear equations. The model developed met every condition listed in the preceding paragraph. Given experimentally measured inlet air properties and cell power data reported by Engel, the model predicted to within one degree Fahrenheit the reported measured temperature of the exit stream. For no heat generation, the velocity profile predicted by the model correlated well with Schlichting's numerical solution for entrance region flow of an incompressible fluid through a duct (9), a less complex problem than the one at hand. The model was therefore considered to have satisfied the original requirements. Full documentation follows.

Modelling Considerations

In this model the focus is on the channel through which air flows over the anode side of the cell. Temperature and concentration gradients in the matrix are represented as variable boundary conditions to the heat and mass transfer equations governing the air stream. The channel has a rectangular cross section, with width much greater than height. Thus, effects of the side walls may be ignored - reducing the problem to one in two dimensions. The channel wall opposite the matrix may be regarded as allowing transfer of neither mass nor heat. Since air humidity is an easily measured quantity, it is employed in the analysis of the mass transfer characteristics of the cell. Changes in humidity may, of course, be directly related to oxygen and hydrogen production. The air, forced into the channel by a fan, enters the channel with a constant velocity field. Wall drag, viscous forces, and heat flux then act to force a non-predetermined velocity field on that air in the channel farther downstream.

It was with a view toward improving the approximation to reality that the present work was begun. There exists no analytic solution to the problem at hand - flow of a compressible fluid through a finite channel with combined heat and mass transfer, and with variable boundary conditions. However, solution by algebraic analysis (solving the finite difference forms of the transport equations) presents no conceptual difficulty. In less than conceptual terms, the problem of determining ways of writing the equations and algorithms which allow solution is somewhat more difficult. The problem becomes then the simultaneous solution of systems of non-linear, inter-related algebraic equations.

Ignoring changes in properties - velocity, density, temperature, etc. - along the width of the flow channel, the system may be described in two dimensions. For the algebraic analysis the channel is divided into volume increments as shown in Figure 1.

In Figure 1, a general volume element (I,J) has length Δx - in the direction of flow, height Δy - perpendicular to flow, and width Δz - into the page. At the walls, the increments (I,1) and (I,N) have heights of $\Delta y/2$. The properties of fluid leaving an element are the same as those properties within the element.

There are N elements across the flow channel, with equally spaced centers. Considering the half-elements (I,1) and (I,N) to be reserved as boundary conditions, there are N-2 sets of total mass, partial mass, momentum, and thermal energy balances around the elements per row I. Assuming that bulk flow is dominant - Graetz number, Reynolds number, and the product of the Reynolds and Schmidt numbers each reasonably greater than unity - one can ignore heat conduction, viscous momentum transport, and diffusion in the direction of bulk flow (the x-direction). This assumption allows balances to be written around element (I,J) using properties of only elements (I,J-1), (I,J), (I,J+1), and (I-1,J). Therefore, knowing the properties of the (I-1) row of elements, the N-2 sets of balances around the elements in row I may be solved simultaneously. Starting with known values - velocity, temperature, and humidity - entering the flow channel (row 0), the values for the N elements in row 1 may be calculated. Knowing the properties of the elements in row 1 allows solution for the values of temperature, velocity, etc. in row 2 and so on until the end of the channel has been reached.

FIGURE 1

Water Vapor Electrolysis Cell Air Flow Channel Showing Increments in the Space Dimensions for Algebraic Analysis of the Transport Equations

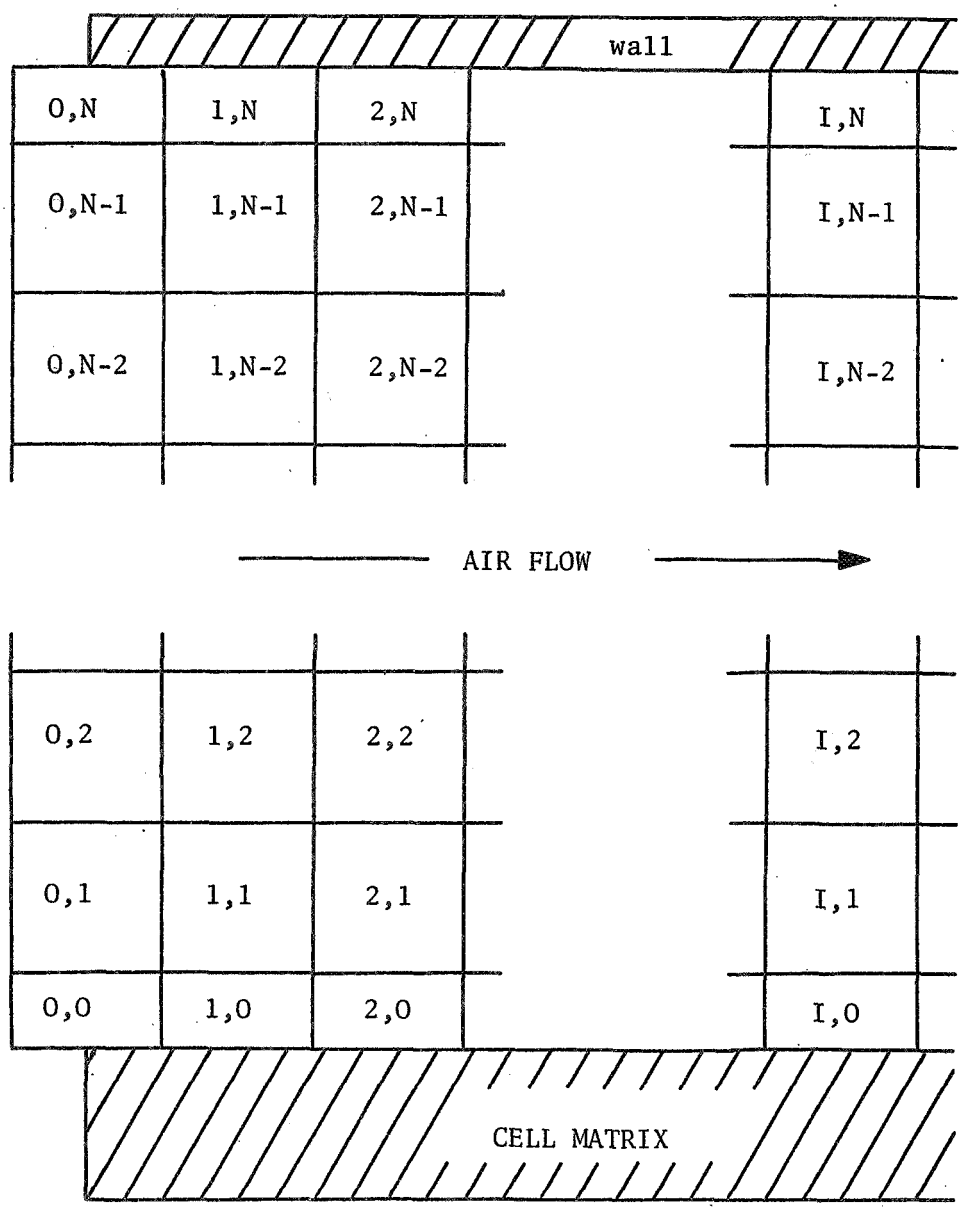

Transport Equations

The mass, momentum, and energy balances around an element (I,J) will be developed in this section. The development is based on that presented in Bird et. al. (1). Nomenclature will be partially included in the discussion below for the sake of clarity, and the full nomenclature is listed at the end of this section.

The starting point is always a rectangular parallelepiped in three-space. Starting from a point (x,y,z) the volume element is bounded x+ Δx, y+ Δy, and z+ Δz. The element is stationary with respect to the axes of the co-ordinate system. As stated previously, there are no property changes in the z direction.

mass balance

The rate of mass flow into the face of the element at x is ($\Delta y \Delta z$) $(pv_x)|_x$. Using similar expressions for flow of mass into and from the other faces of the element, the following equation holds at steady state:

$$(\Delta y \Delta z)\ ((\rho v_x)|_x - (\rho v_x)|_{x+\Delta x)} + (\Delta x \Delta z)\ ((\rho v_y)|_y - (\rho v_y)|_{y+\Delta y)} = 0$$

Defining the following quantities

ρ_o = density of air entering flow channel

v_o = x-velocity of air entering flow channel

m = $\Delta y/\Delta x$

U = v_x/v_o

V = v_y/v_o

RHO = ρ/ρ_o,

the mass balance becomes

$$mRHO(I-1,J)U(I-1,J) - mRHO(I,J)U(I,J)$$
$$+ RHO(I,J-1)V(I,J-1) - RHO(I,J)V(I,J) = 0.$$

momentum balance

The net flow of x-momentum into the element by bulk flow is

$$(\Delta y \Delta z)\ ((\rho v_x v_x)|_x - (\rho v_x v_x)|_{x+\Delta x})$$
$$+ (\Delta x \Delta z)\ ((\rho v_y v_x)|_y - (\rho v_y v_x)|_{y+\Delta y}).$$

The net flow of x-momentum into the element by molecular transport is

$$(\Delta x \Delta z)\ (\tau_{yx}|_y - \tau_{yx}|_{y+\Delta y}).$$

The resultant pressure force in the x-direction is

$$(\Delta y \Delta z)\ (p|_x - p|_{x+\Delta x}).$$

For a Newtonian fluid $\tau_{yx} = -\mu \dfrac{\partial v_x}{\partial y}$.

Using the quantities defined above, the dimensionless momentum balance is then the following, about a general volume element (I,J):

$$mRHO(I-1,J)U(I-1,J)^2 - mRHO(I,J)U(I,J)^2$$
$$+ RHO(I,J-1)V(I,J-1)U(I,J-1) - RHO(I,J)V(I,J)U(I,J)$$
$$+ (\mu/(\Delta y \rho_o v_o)(U(I,J-1) - 2U(I,J) + U(I,J+1))$$
$$+ (m/(\rho_o v_o^2))(p(I-1) - p(I)) = 0$$

In the above equation pressure is written as a function of x only.

thermal energy balance

The net convective heat flow into the element is

$$(\Delta y \Delta z)((\rho c_v v_x t)|_x - (\rho c_v v_x t)|_{x+\Delta x})$$

$$+ (\Delta x \Delta z)((\rho c_v v_y t)|_y - (\rho c_v v_y t)|_{y+\Delta y}).$$

where t is absolute temperature.

The net flow of heat into the element by conduction is

$$(\Delta y \Delta z)((q_y|_y - q_y|_{y+\Delta y}).$$

The internal energy increase in the element due to compression is

$$(\Delta y \Delta z)((pv_x)|_{x+\Delta x} - (pv_x)|_x)$$

$$+ (\Delta x \Delta z)((pv_y)|_{y+\Delta y} - (pv_y)|_y).$$

By Fourier's law, $q_y = -k \frac{\partial t}{\partial y}$.

Since neither thermal conductivity -k- nor heat capacity $-c_v-$ is a particularly strong function of temperature, they are considered constants in this model. Introducing the following quantities

t_o = temperature of entering air

$T = t/t_o$,

the dimensionless thermal energy balance is

$$mRHO(I-1,J)U(I-1,J)T(I-1,J) - mRHO(I,J)U(I,J)T(I,J)$$

$$+ RHO(I,J-1)V(I,J-1)T(I,J-1) - RHO(I,J)V(I,J)T(I,J)$$

$$+ (K/)\Delta y \rho_o v_o c_v))(T(I,J-1) - 2T(I,J) + T(I,J+L))$$

$$+ (p(I)/(\rho_o c_v t_o))(mU(I,J) - mU(I-1,J) + V(I,J)$$

$$- V(I,J-1))$$

$$= 0$$

For pressure in dyne/cm^2 the last term in the above equation must be divided by the conversion factor 4.13×10^7, to get the proper units, in the cgs system.

partial mass balance

The final required balance is a water vapor balance around the increment. Since the water vapor content of the air is so small, it is essentially the density of the air alone, and the mass fraction of water is essentially its humidity -h- expressed in g water/g dry air. Thus the net flow of water vapor into the element by convection is

$$(\Delta y \Delta z)((h\ v_x)|_x - (h\ v_x)|_{x+\Delta x}) + (\Delta x \Delta z)((h\ v_y)|_y - (h\ v_y)|_{y+\Delta y}).$$

The net flow of water vapor into the element by diffusion is

$$(\Delta x \Delta z)\ (\ j|_y - j|_{y+\Delta y}).$$

By Fick's law, $j = D\ \frac{\partial(h)}{\partial y}$.

Introducing the quantities h_o = humidity of entering air stream, and $H = h/h_o$, the dimensionless partial mass balance is

$$mH(I-1,J)RHO(I-1,J)U(I-1,J) - mH(I,J)RHO(I,J)U(I,J) + H(I,J-1)RHO(I,J-1)V(I,J-1) - H(I,J)RHO(I,J)V(I,J) + (D/(\Delta y v_o)(H(I,J-1)RHO(I,J-1) - 2H(I,J)RHO(I,J) + H(I,J+1)RHO(I,J+1)\ ) = 0$$

To solve the above-developed equations the number of unknowns must equal the number of available equations. Considering all the properties of all the elements in row I-1 known, there are 5N+1 unknowns to be solved for in row I. They are

U(I,J) J=1,N

V(I,J) J=1,N

RHO(I,J) J=1,N

T(I,J) J=1,N

H(I,J) J=1,N

p(I)

With mass, momentum, thermal energy, and partial mass balances around each of the N-2 full elements in row I, there are now 4N-8 equations. Boundary conditions at the walls of the channel yield two more equations each for U,V,T, and H. The ideal gas law may be applied to the air stream at normal operating conditions, and $\rho = Mp/Rt$ adds N equations. A momentum balance at the wall yields one more equation, for the pressure drop from row I-1 to row I. Thus there are sufficient equations to solve for the unknown values. The usual assumption of no slip at the walls yields four of the boundary condition equations:

$$U(I,1) = 0$$

$$V(I,1) = 0$$

$$U(I,N) = 0$$

$$V(I,N) = 0$$

Since no heat or mass crosses the wall opposite the matrix, two more boundary condition equations may be used:

$$T(I,N) = T(I,N-1)$$

$$H(I,N) = H(I,N-1).$$

To determine the matrix-side boundary conditions for temperature and humidity, it is necessary to make balances around the matrix, assuming no interaction with the exit hydrogen stream.

The heat generated by electrolysis is large with respect to the latent heat changes and the heat of solution due to water's entering the matrix from the air stream. Thus, the heat generated by the electrolysis process is the heat crossing the matrix-channel interface. This generated heat -Q- is $(\Delta x \Delta z)(0.239i(E - E_o))$, in cal/sec, where

i = cell current density

E = operating cell voltage

E_o = cell reversible emf.

The heat entering the air stream at element (I,1) is

$$Q = k(\Delta x \Delta z/\Delta y)(t(I,1) - t(I,2))$$

$$= (k\Delta x \Delta z t_o/\Delta y)(T(I,1) - T(I,2)).$$

Since the heat generated is equal to the heat leaving the matrix,

$$T(I,1) = T(I,2) + 0.239i(E - E_o)\Delta y/(kt_o).$$

Water leaves the matrix by electrolysis, a process consuming 9.334×10^{-5} g water/amp-sec. Water enters by diffusion at a mass flow rate of

$$D(\Delta x \Delta z/\Delta y)(h(I,2)\rho RHO(I,2) - h(I,1)\rho RHO(I,1)).$$

Equating water in with water removed at steady state, one gets the final boundary condition:

$$H(I,1) = (H(I,2)RHO(I,2) - 9.334 \times 10^{-5} i\Delta y/(\rho_o h_o D))/RHO(I,1)$$

Cell current density is properly a function of the temperature and acid concentration of the cell matrix. Due to a lack of physical properties of sulfuric acid in the gel matrix, there was a choice of using the vapor pressure and resistivity of sulfuric acid itself or of assuming the current density is constant and equal to the cell current load divided by the product of the length and width of the cell. In the work thus far, the latter was chosen for the sake of simplicity.

The pressure drop from row I-1 to row I is determined by a momentum balance at the wall, where v_x and v_y are identically zero. Here the equation of motion reduces to

$$\frac{\partial p}{\partial x} = \frac{dp}{dx} = \mu \frac{\partial^2 vx}{\partial y^2}$$

Using the three-point Lagrange interpolating polynomial, the second derivative evaluated at the wall is

$$\frac{\partial^2 vx}{\partial y^2} = (v_x(I,1) - 2v_x(I,2) + v_x(I,3))/(\Delta y)^2$$

The first order approximation of dp/dx is

$$(p(I) - p(I-1))/\Delta x.$$

Therefore,

$$p(I) = p(I-1) + v_0 \mu \Delta x(- 2U(I,2) + U(I,3))/(\Delta y)^2$$

Solution of the Transport Equations

general

The equations presented in the previous section are non-linear, interdependent algebraic equations, and must be solved simultaneously. An iterative technique is necessary for the solution of these equations. The various popular algorithms for the solution of systems of non-linear equations were tried, and they failed to yield solutions. Perhaps further work would have led to a solution in one or more cases, but the vast number of arithmetic operations involved in these methods would have made the solution prohibitively expensive. For example, one iteration using the popular Newton method - block modified to cut down on storage and number of operations performed -

required five seconds of execution time on an IBM Operating System/360 high-speed digital computer.

Finally the methods for the simultaneous solution of systems of non-linear algebraic equations were discarded. Viewing specific variables as "transitory constants" allows one to use the methods of linear equation problem solving. Since these transitory constants must be given numerical values for digital computer solution, the algorithm must be iterative.

Consider that the system of equations to be solved is of the form Ax=b, where x is a vector composed of all the unknowns in row I - the vectors U,V,T and the scalar p. A is the matrix of coefficients of x which may be either constants or the "transitory constants" - components of the vectors U,V,T and RHO. The vector b is composed of all terms in the equations that are not coefficients of the vector x. The obvious choice for the transitory constants in matrix A and vector b are those values of the elements of the x vector calculated in the previous iteration. As the algorithm converges to a solution - x vectors from succeeding iterations becoming identical - the transitory constants in A and b become their true values and not just approximations of these values.

While the specific iterative algorithm used in this model - described later in this section - was not found in the literature, the method - a combination of direct and indirect algorithms - can best be described as block-iterative Seidel. Seidel iteration can guarantee that, guessing a solution vector x^c for the system Ax=b, one iteration will generate another solution vector x^{i+1} that is closer to the true solution x than was x^i. The generally used criterion for this convergence is the diagonal dominance of the matrix A.

Diagonal dominance is defined as the condition whereby the sum of the absolute values of the off-diagonal elements in a row or column of the matrix is less than the absolute value of the element on the diagonal. Since, in this model, the matrix A is made up of transitory constants, and the form of the matrix varies with each iteration and with distance along the flow channel, there is the possibility that it will lose its diagonal dominance at some time during computation. In such an instance the rather simple expedient of pre-multiplying both sides of Ax=b by the transpose of A will guarantee convergence to a solution - if one exists. This "simple expedient" - forming a symmetric positive-definite coefficient matrix - is to be generally avoided if at all possible. It causes computation time to be more than cubed, it doubles storage requirements, and it alters any useful form properties that the matrix A might have had. In the algorithm for this model - discussed next - the matrix A has indeed some useful form properties, allowing great savings in computation time and storage requirements.

specific

In the mass balance around element (I,J), regard everything as a transitory constant except the terms of the V vector - V(I,J-1) and V(I,J). The mass balances may then be written in the form

$$a_J V(I,J-1) + b_J V(I,J) = bb_J; \quad J=2,N-1$$

which is linear in V and where the coefficients a, b, and bb are composed of actual or transitory constants:

$$a_J = RHO(I,J-1)$$

$$b_J = RHO(I,J)$$

$$bb_J = mRHO(I,J)U(I,J) - mRHO(I-1,J)U(I-1,J)$$

If written in the form Ax=b, x would be the V vector, b would be the bb vector, and the A matrix would be composed of elements on the diagonal-b_J, elements on the lower off-diagonal - a_J, and zeros everywhere else. The algorithm for the solution of this system of equations is particularly simple:

$$V(I,1) = 0 \quad \text{(boundary condition)}$$

$$V(I,J) = (bb_J - a_J V(I,J-1))/b_J;\ J=2,N-1$$

From this most recent approximation of the V vector, and the approximations of p, RHO, and T, the momentum balances for row I may be solved to yield a new approximation of the U vector. The $U(I,J)^2$ term in the momentum balance poses a problem, however, making the equation non-linear in U. The obvious ruse of writing the term as U(I,J)U(I,J) and considering the first U(I,J) as a transitory constant coefficient of the second does not fool the algorithm one bit. It generates either of the two mathematically possible answers that a quadratic equation may have. The $U(I,J)^2$ term was thus expanded in its Taylor series about the known point U(I-1,J):

$$U(I,J)^2 = U(I-1,J)^2 + 2U(I-1,J)(U(I,J)-U(I-1,J)) + (U(I,J)-U(I-1,J))^2.$$

Dropping the last term yields a linear approximation of $U(I,J)^2$ that is accurate to within $(U(I,J)-U(I-1,J))^2$. Under normal operating conditions of the cell, U is on the order of 10^0, and computer output of the model under these normal operating conditions shows that (U(I,J)-U(I-1,J)) is always less than 10^{-2}. The error introduced by linearization is then less than 0.01 percent.

The momentum balances are now linear in U and may be written as follows:

$$a_J U(I,J-1) + b_J U(I,J) + c_J U(I,J+1) = bb_J;\ J=2,N-1.$$

$$a_J = \mu/(\Delta y \rho_o v_o) + RHO(I,J-1)V(I,J-1)$$

$$b_J = -2\mu/(\Delta y \rho_o v_o) - RHO(I,J)V(I,J) - 2mRHO(I,J)U(I-1,J)$$

$$c_J = \mu/(\Delta y \rho_o v_o)$$

$$bb_J = -mRHO(I-1,J)U(I-1,J)^2 - mRHO(I,J)U(I-1,J)^2 - (m/(\rho_o v_o^2))(p(I-1) - p(I))$$

Since U(I,1) and U(I,N) are zero (boundary condition), writing the equations in the form Ax=b - with N set at 7, for purposes of example - would yield the following matrix equation:

$$\begin{vmatrix} b_2 & c_2 & 0 & 0 & 0 \\ a_3 & b_3 & c_3 & 0 & 0 \\ 0 & a_4 & b_4 & c_4 & 0 \\ 0 & 0 & a_5 & b_5 & c_5 \\ 0 & 0 & 0 & a_6 & b_6 \end{vmatrix} \times \begin{vmatrix} U(I,2) \\ U(I,3) \\ U(I,4) \\ U(I,5) \\ U(I,6) \end{vmatrix} = \begin{vmatrix} bb_2 \\ bb_3 \\ bb_4 \\ bb_5 \\ bb_6 \end{vmatrix}$$

The coefficient matrix in the above equation is tridiagonal in form. This allows a saving in both storage space and computation time. In the first case, although the matrix is actually of size (N-2) x(N-2), it may be stored in an array of dimensions (N-2)x3 - avoiding taking up storage space with a great number of zeros. Also there is a special algorithm based on Gaussian elimination that solves tridiagonal systems a great deal faster than those methods used for solving general systems of equations. Computation time is directly proportional to the number of elements in the "unknown" vector - here, N-2 - rather than to its square or cube.

The algorithm is the following, the operations done sequentially:

$$c_2 = c_2/b_2$$

$$bb_2 = bb_2/b_2$$

$$c_J = c_J/(b_J - a_J c_{J-1})$$

$$bb_J = (bb_J - a_J bb_{J-1})/(b_J - a_J c_{J-1});\ J=2,N-1$$

$$U(I,N-1) = bb_{N-1}$$

$$U(I,J) = bb_J - c_J U(I,J+1):\ J=N-2,N-3,\ldots,1$$

The energy equation may be written as a tridiagonal system of equations linear in T, with the transitory constants the new approximations of the V and U vectors and the values of the RHO vector and p taken from the previous iteration. The new approximation of the T vector may be calculated in the same manner as was the U vector in the preceding step. The pressure may then be calculated from the wall momentum balance, and RHO may be then calculated from the new approximations of p and T by use of the ideal gas law.

If the new approximations of the vectors V, U, and T are sufficiently close to the corresponding vectors generated in the previous iteration, the algorithm has converged to a solution. The (I+1)th row is then operated on, using the vectors V,U,T, and RHO and p for row I as the initial values of the transitory constants. If the new approximations are not reasonable facsimiles of the vectors generated by the preceding iteration, these new vectors become the next values taken on by the transitory constants for the equations of row I, and the process is repeated until convergence is reached.

Since the water vapor content of the air is so small, it exerts negligible effect on the air's other properties. Indeed, the partial mass balances are the only equation in which H appears. Thus no purpose is served by including it in the iteration loop. The partial mass balances are, then, solved for the H vector only after convergent solutions to U, V, and T have been attained.

The above algorithm, in physical form, is a subroutine written in Operating System/360 FORTRAN IV Language, G, H, or Watfor compilers. The routine is self-contained, requiring input of only the dimensions of the cell, properties of the air stream entering the cell, and the number of increments per row desired. As a convergent solution is attained for a given row I, the routine causes that solution to be printed out. The calling program links with the subroutine by the FORTRAN statement

```
CALL AMBA1(N,CONST)
```

The calling program must dimension N as an INTEGER*4 variable, N being the number of elements in a row I. CONST is a REAL*8 array of size 14, and contains the rest of the information required by the routine. The elements of CONST are the following:

CONST(1) = L = length of cell, cm

CONST(2) = W = height of flow channel, cm

CONST(3) = M = $\Delta y/\Delta x$

CONST(4) = PO = initial pressure, atm

CONST(5) = TO = initial temperature, ^{o}K

CONST(6) = VO = initial velocity, cm/sec

CONST(7) = HO = initial humidity, g water/g dry air

CONST(8) = IDEN = cell current density, amp/cm^2

CONST(9) = E = cell operating voltage, volt

CONST(10) = MU = average air viscosity, g/cm-sec

CONST(11) = K = average air thermal cond., cal/cm-sec/^{o}K

CONST(12) = D = average air diffusivity, cm^2/sec

CONST(13) = CV = average air heat capacity, cal/g-^{o}K

CONST(14) = MW = molecular weight of air, g/g-mol

Results

Iterative solutions in general - and solutions for non-linear equations in particular - are quite temperamental, working well in some instances, converging so slowly as to be prohibitively expensive in time and money in others, but most frequently not converging at all. Thus, the routine was first checked out as to its region of convergence with respect to two major design variables - initial velocity of the air stream and heat generated by electrolysis. Initial pressure and temperature were held constant at 1 atm and 298^{o}K, respectively, and various combinations of velocity and heat load were tested for ability of the algorithm to lead to a solution. For generality, they are in the form of dimensionless groups, which appeared as a result of making the balances dimensionless. They are a Reynolds number, defined as $\Delta y v_o \rho_o / \mu$; and a dimensionless heat load, DIMQ, defined as mQ/kt_o.

To give the reader a feel for these values, consider the following normal operating conditions for the cell. Air at room temperature and atmospheric pressure flows through a slit of height 0.159 cm, with N=7 (y = 0.0265 cm). RE would then be 31.43. At an operating current density of 20 amp/ft^2, DIMQ = 0.00625 RE. In Figure 2 the region of convergence with respect to these two variables is presented graphically. The ratio m is its generally used value of one.

FIGURE 2

Region of Convergence to a Solution

for Math Model of Water Vapor Electrolysis Cell

as a Function of Electrolysis Rate and Entrance Air Velocity

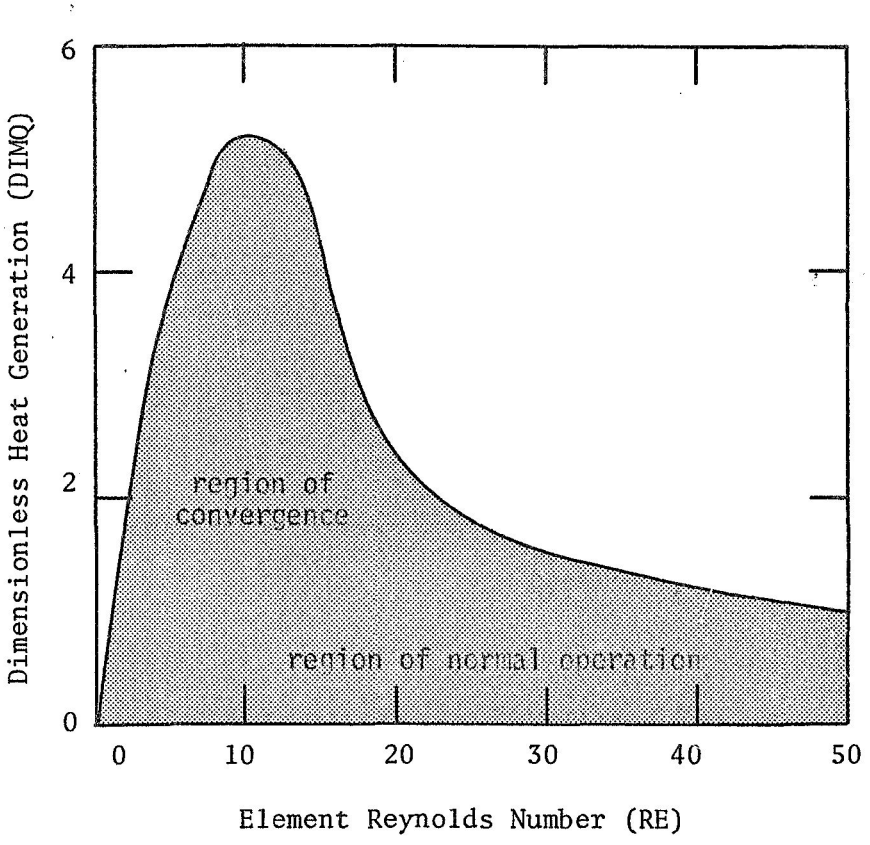

Figure 2 shows that the algorithm causes convergence to a solution in the normal operating region of the cell. Physical limitations of the model account for at least a portion on the region where convergence will not occur. At low Reynolds number, the assumption of bulk flow dominance is no longer valid. At a high Reynolds number, viscous dissipation - a term ignored in the thermal energy equation - becomes significant at low heat load. Under high heat load to the system, the assumption of negligible heat conduction in the x-direction also breaks down. Beyond these observations, the algorithm itself and the changing form of the coefficient matrix are responsible for the restricted regime of convergence. Indeed, there appears to be an effect of element size on convergence. As the size of the element is decreased, computation time skyrockets for all else constant. This is not to say that, in the limit as element size approaches zero, the equations do not become the proper partial differential equations. It is rather to acknowledge the temperament of algorithms for the solution of non-linear systems of equations.

The last test of the model to date is against experimental data, reported by Engel(8). Normal operating conditions entered into the subroutine, converted to cgs from the reported engineering units were the following:

L	= 4.75 cm	IDEN	= 0.0215 amp/cm^2
W	= 0.159 cm	E	= 2.135 volt
m	= 1.0	MU	= 0.0002 g/cm-sec
PO	= 1.0 atm	K	= 0.0000662 cal/cm-sec-^oK
TO	= 298 ^oK	D	= 0.220 cm^2/sec
VO	= 200 cm/sec	CV	= 0.165 cal/g-^oK
HO	= 0.02 g water/g air	MW	= 29.0

The temperature of the air at the exit of the flow channel was reported to be 83°F by Engel. The present model predicted an average exit temperature of 82°F. The Clifford model discussed earlier reported an exit temperature for about these same conditions, but with a cell voltage of 2.34 volt. Since the Clifford model assumes constant air properties, multiplying his reported air temperature rise of 7.8°F by the ratio (2.135/2.34) would yield a reasonable approximation of the exit temperature that would be predicted by the Clifford model at the experimental conditions reported by Engel. That value is 7.1°F, for an exit temperature of the air stream of around 83°F. Thus, the present model is in good agreement with the data reported by both previous investigators. However, the present model predicts this exit temperature, while the Clifford and Engel models require experimental determination.

The velocity profiles assumed by the Clifford and Engel models were parabolic and flat-parabolic, respectively. Figure 3 shows the velocity profiles predicted by the present model in the entrance region of the flow channel at the above conditions, and the profile at the end of the channel. The horizontal axis is in units of y/W, the fraction of the height of the flow channel above the cell matrix. The vertical axis is in terms of U, the dimensionless x-velocity. The parameter is x/W, the ratio of the distance along the flow channel to the height of the flow channel.

Figure 3 shows a slight but noticeable skew effect in the velocity distribution, with higher velocity on the matrix side of the channel than at a corresponding distance from the adiabatic wall. This is due to the heating effects on the air near the matrix wall - lowering density, thus increasing velocity. At higher heat loads -

FIGURE 3

Velocity Profiles of Air in

the Flow Channel at Typical Conditions

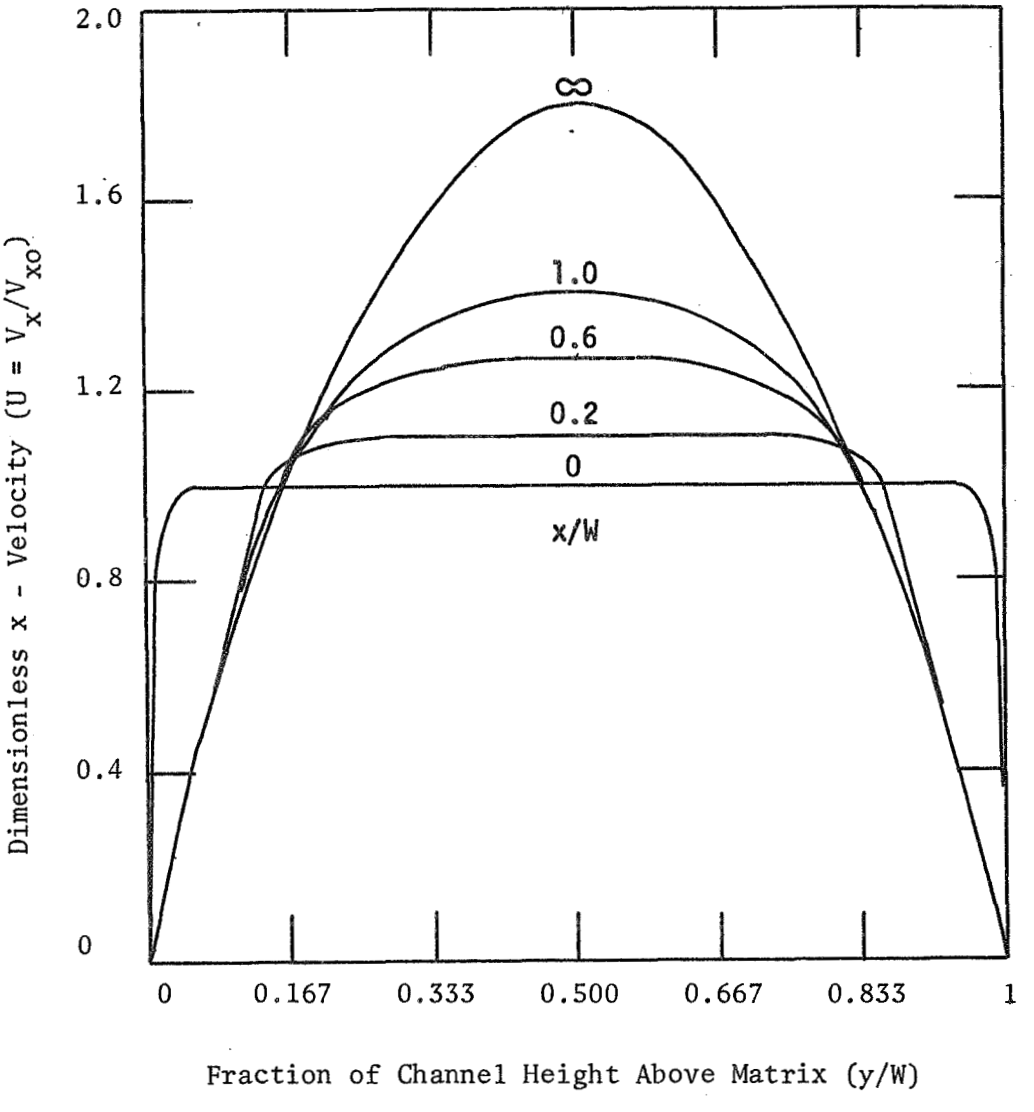

much higher than those at normal operating conditions - the deformation of the velocity profile from symmetry about the center line of the channel becomes quite pronounced.

It is also evident that a flat velocity profile at the entrance region of the cell is a good approximation of a reality only for quite short distances down the channel, indeed less than one channel width of distance. Neither is a fully developed parabolic velocity profile a reasonably accurate one. The Bloom model of the cell under the above normal operating conditions predicts that fully developed flow begins about seven eighths of the distance down the channel.

Conclusions and Recommendations

The ideal model would operate in the time as well as space domain. The physical and electrochemical properties of the electrolysis medium should be integrated into the model, and transport equations developed for the matrix. Such a model would have much greater utility than any of the three presently available ones. For example, the problems of start-up could be investigated, especially with regard to flooding or drying of the matrix. The utility of modelling for non-hazardous systems does not lie in steady state solutions, but rather in predicting response to perturbations and in gathering data impossible or difficult to measure.

Conceptually, extending the present model to three dimensions and integrating the physical chemical data gathered in the present work presents no problem. The problem is physical. The present model, with only seven space increments across the width of the flow channel requires the solution of thirty-five simultaneous non-linear algebraic equations for each space increment along the length of the channel.

The time required for one solution on an IBM System/360-67 is on the order of one minute. Adding the time dimension would increase computing time enormously. Adding descriptive equations for the cell matrix would not have as great an effect.

It is recommended that the excellent time-integration capability of the analog computer be utilized in the further development of the model of the water vapor electrolysis cell. Storage and switching considerations dictate using a digital/analog hybrid computer. Such a computer has become available at the University as of this writing.

Nomenclature

c_v	heat capacity at constant volume cal/g^{o}K
D	diffusivity cm^2/sec
h	humidity g water/g air
I	cell current amp
i,IDEN	cell current density amp/cm^2
k	thermal conductivity cal/cm-sec-^{o}K
L	cell length cm
MW	molecular weight of air
p	absolute pressure atm
R	gas law constant cm^{3}atm/g-mol ^{o}K
v	velocity cm/sec
VOLT,E	cell voltage volt
W	height of flow channel cm
t	absolute temperature ^{o}K

subscripts

o	evaluated at the cell entrance
x	x-component of a vector
y	y-component of a vector

(I,J)	evaluated at increment (I,J)
greek	
Δx	length of element cm
Δy	height of element cm
Δz	width of element cm
μ	viscosity g/cm sec
ρ	density g/cm^3
dimensionless quantities	
H	h/h_o
m	$\Delta y/\Delta x$
RHO	ρ/ρ_o
T	t/t_o
U	v_x/v_o
V	v_y/v_o

PHYSICAL-CHEMICAL STUDIES OF THE WATER VAPOR CELL ELECTROLYSIS MEDIUM

General Introduction

Physical-chemical properties of the electrolysis cell matrix - a nominal mixture of 10 wt% CAB-O-SIL M5 amorphous silica in 60 wt% aqueous sulfuric acid - influence the operation of the cell. Water vapor is absorbed from the air stream as a function of the equilibrium partial pressure of water of the matrix. Both ionic transport and heat dissipation in the cell matrix depend on the resistivity of matrix material. The following sections report the results of experimental work investigating those two physical-chemical properties of systems of CAB-O-SIL M5 and sulfuric acid.

Equilibrium Relative Humidity of Mixtures of CAB-O-SIL M5 and Sulfuric Acid

introduction

The humidity in equilibrium with the silica-sulfuric acid matrix is the controlling factor in the electrolysis cell's water absorption capability. Should addition of silica to sulfuric acid change the partial pressure of water vapor over the acid, the mass transfer aspects of cell operation would be affected. The present work was undertaken to determine any such effects.

procedure

Known mixtures of CAB-O-SIL M5 and sulfuric acid were prepared and the equilibrium partial pressures of water vapor measured. Relative humidity (RH) was chosen as the dependent variable to be measured, being convenient to obtain. Since relative humidity over sulfuric acid is only

mildly temperature dependent, stringent thermostating was not required.

Mixtures in the range of zero to ten weight percent CAB-O-SIL M5 in approximately sixty weight percent sulfuric acid were prepared. A mixture was allowed to come to equilibrium in a sealed container into which was inserted a precision hygrosensor*. A constant relative humidity over a twenty-four hour span was taken to indicate the attainment of equilibrium. The apparatus used in this experiment is shown schematically in Figure 4. In Figure 4 the components are the following:

1. Airtight test chamber containing silica-acid mixture
2. Narrow range precision hygrometer*
3. Small pump for circulation of air within the test chamber
4. Temperature-Humidity Indicator*

initial experimental results

The first series of measurements was made during the period 16 to 25 September 1969. A base of sulfuric acid was placed in the test chamber and its equilibrium RH measured. Weighed samples of CAB-O-SIL M5 were added sequentially, and the equilibrium RH over each mixture was measured in turn. The results are presented in Figure 5.

The results presented in Figure 5 show relative humidity to have a striking dependence upon the silica content of the mixture. That increase in the partial pressure of water vapor would have a quite adverse effect on cell operation. Were an electrolysis unit designed on the basis of equilibrium humidity over sulfuric acid alone,

---

*Model 15-3001 Hygrometer Indicator; Hygrodynamics, Inc; Silver Spring, Md.

FIGURE 4

Experimental Apparatus for the Measurement of

Equilibrium Relative Humidity of Mixtures of Sulfuric Acid

and CAB-O-SIL M5 Silica

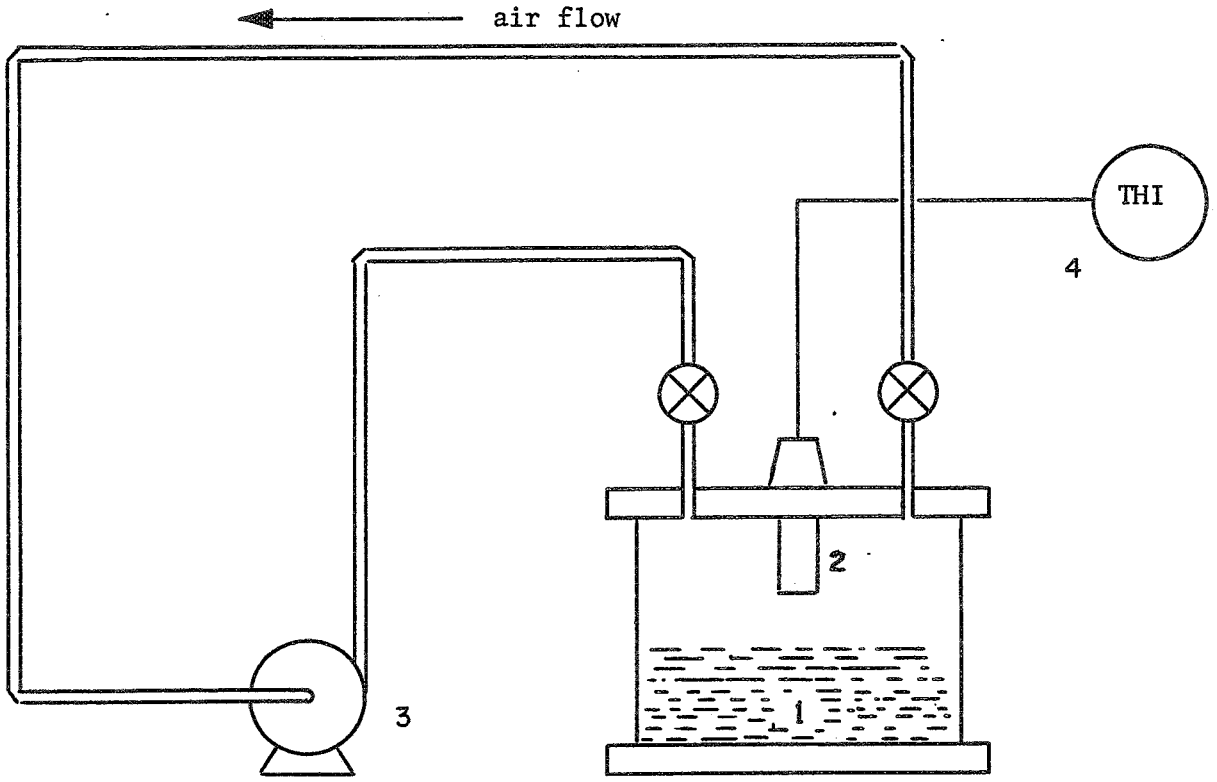

FIGURE 5

Equilibrium Relative Humidity of Mixtures of 60 wt% Sulfuric Acid and CAB-O-SIL M5 Silica, Trial 1, 16-25 September 1969

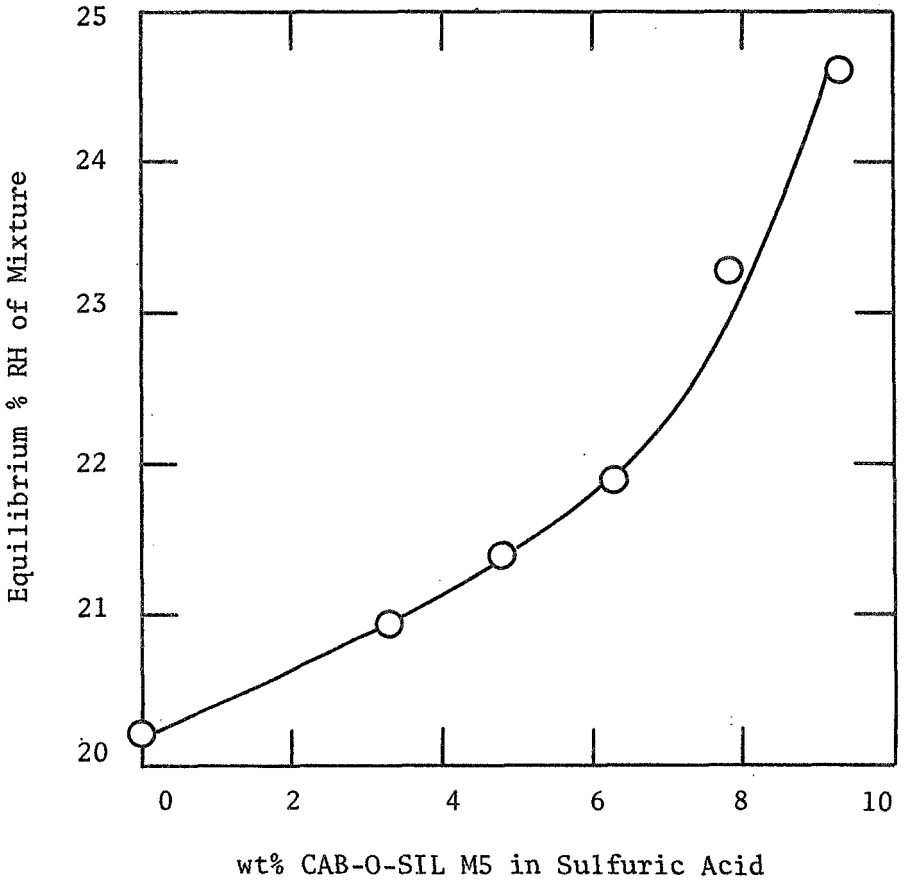

insufficient water vapor would have been absorbed from the air stream. The matrix would dry up, and the unit would fail. The matter thus deserved further study.

The hypothesis advanced to account for this increase in humidity with CAB-O-SIL M5 addition was the following. Since the silica was stored in an open container, it adsorbed water from the atmosphere. Upon mixing with sulfuric acid, the silica released its physically adsorbed water, diluting the bulk liquid and raising the mixture's equilibrium relative humidity. A second possibility would have been the dehydration of the silanol sites on the silica surface. Since only heat to ca. 900 degree Fahrenheit and neutralization with a base have been mentioned (6,12) as methods of doing so, the possibility has not been more deeply investigated.

As a preliminary test of the hypothesis, ambient humidity data for the period of expermental work was requested of the Meteorological Observatory, The Pennsylvania State University. From the beginning of the work on 16 September through 19 September, ambient RH at the times of mixing were between 50 and 55 percent. At the time the 8 percent CAB-O-SIL mixture was prepared on 20 September the RH was 60 percent. The last mixture - 9.24 % CAB-O-SIL - was prepared while the ambient humidity was 70 percent. Figure 2 shows that the RH curve took on an increasing slope for the last two data points. This indicated that the humidity over the stored silica could have exerted an effect on the RH over the silica-acid mixture.

On the above basis, the hypothesis was chosen for further investigation. Information was thus required for the water vapor adsorption of CAB-O-SIL M5. The gathering of such information is the subject of the next section.

Equilibrium Water Vapor Adsorption of CAB-O-SIL M5

introduction

In the previous section, addition of CAB-O-SIL M5 exposed to high ambient relative humidity was shown to increase the equilibrium relative humidity of sulfuric acid. In explanation, the hypothesis put forward was that the silica had sufficient water content to cause a dilution of the sulfuric acid, raising the mixture's equilibrium vapor pressure. To test the hypothesis, a knowledge of the amount of water adsorbed by the CAB-O-SIL M5 as a function of humidity was required.

Two conflicting sources of information were available - data supplied by the manufacturer, Cabot Corporation, and Young's comprehensive silica-water vapor study (12). The manufacturer supplied an adsorption isotherm showing the lack of hysteresis characteristic of non-porous adsorbents. A thirty minute attainment of equilibrium was reported (4). Young reported agreement with the above up to a relative humidity of 40%. Above that, equilibrium time rose to several hours and hysteresis was observed on desorption. Young reports that cycling - adsorption followed by desorption - decreased the area of the hysteresis loop. After a half dozen cycles, the adsorption and desorption curves coincided, the resultant curve showing an isotherm displaced considerably upward from the original adsorption isotherm. The displacement began at a relative humidity of about 40%.

The non-porous amorphous silica that is CAB-O-SIL M5 should show no adsorption-desorption hysteresis. There should be only one equilibrium isotherm at 75 degree Fahrenheit. The present experimental water vapor adsorption study was initiated to clarify the situation.

procedure

The purpose of the experiment was the measurement of the adsorption equilibrium between CAB-O-SIL and atmospheric water vapor. The amount of water adsorbed onto, or desorbed from, the CAB-O-SIL is conveniently measured gravimetrically. The amount of water vapor in the air may be determined with an accurate hygrometer. A constant relative humidity may be obtained over a sulfuric acid solution of fixed concentration. Interest lay in the region of ambient temperature and pressure, so no special requirement was made to control those parameters.

Given the above requirements, the apparatus sketched in Figure 6 was assembled. Having used available components, the system consisted of two parts, linked by tubing. Those two parts were an adsorption chamber and a constant humidity chamber.

The adsorption chamber was an enclosed vertical glass cylinder in which hung a quartz spring. Suspended from the spring was a small bucket containing the CAB-O-SIL sample. The amount of water gained or lost by the sample was measured by the extension or contraction of the spring using a cathetometer.

The humidity chamber was a section of Pyrex pipe capped at both ends. In the bottom lay approximately one liter of sulfuric acid solution for maintenance of constant relative humidity in the two chambers. Inserted into the chamber was a temperature-humidity sensing probe.

A small pump was used to circulate air between the two chambers. The air passed over the sulfuric acid solution, left the humidity chamber to contact the sample in the adsorption chamber, and returned to the humidity chamber to close the loop.

FIGURE 6

Experimental Apparatus for the

Measurement of the Equilibrium Water

Vapor Adsorption of CAB-O-SIL M5 Silica

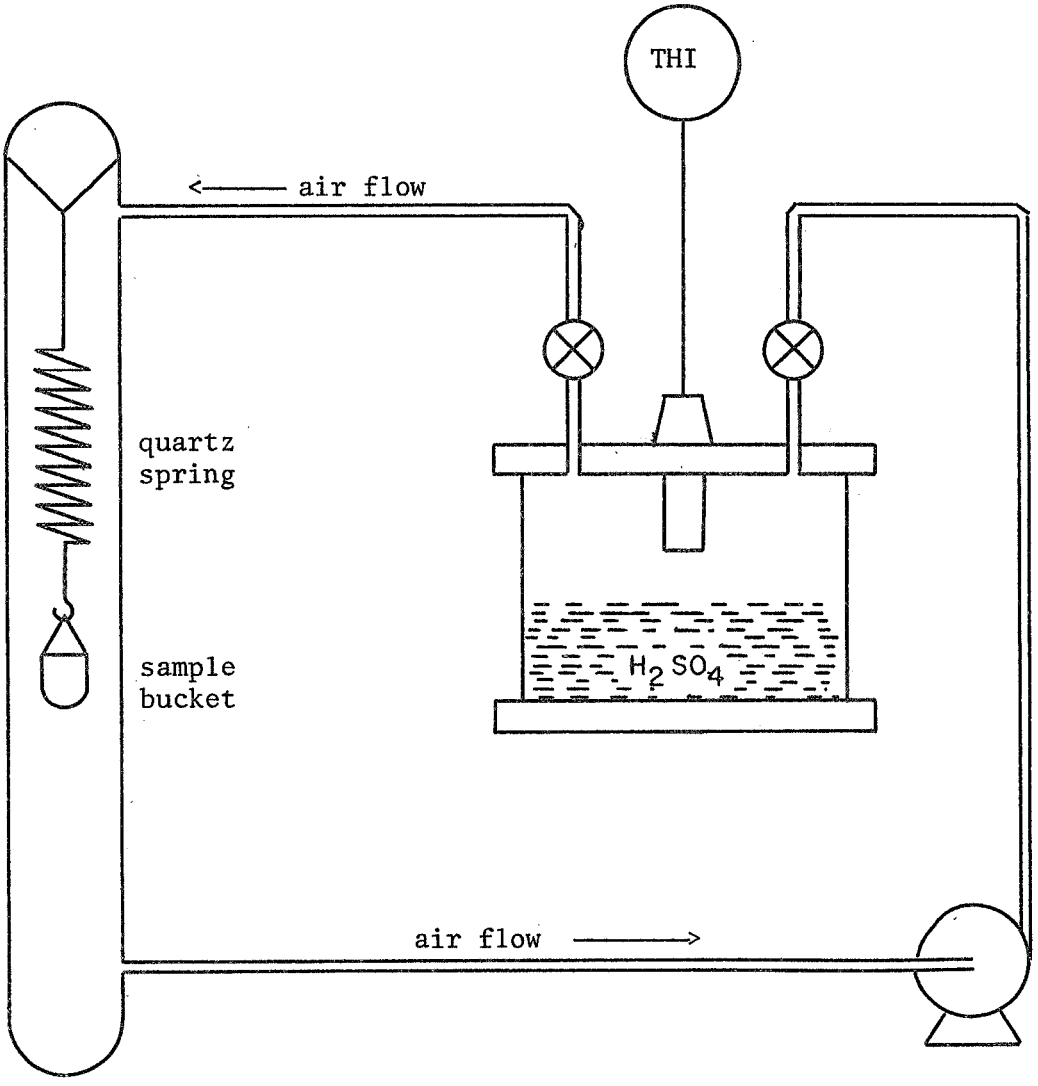

The plan of the experiment was quite simple and direct. Upon calibration of the analytical instruments, the quartz spring and the temperature-humidity indicator, an empty sample bucket was to be suspended from the spring and its elevation noted via the cathetometer. A sample was then to be placed in the bucket, the bucket again suspended from the spring, and the adsorption chamber sealed airtight. A solution of sulfuric acid was then to be placed in the humidity chamber, and the appropriate sensor for the temperature-humidity indicator* inserted through the top plate, which was then bolted down, sealing the system. Equilibrium was to be considered attained after the elevation of the spring had remained constant for one day. Upon attainment of equilibrium, valves in the connecting tubing were to be closed, isolating the adsorption chamber, and the humidity chamber unsealed. The solution in the chamber was then to be either diluted or concentrated to yield a different desired humidity, and the system resealed.

The requirement of constant mass for a one-day period reflected a suspicion concerning the data reported by both Cabot and Young. While the surface adsorption may be essentially instantaneous, diffusion of water vapor into the bulk of the sample certainly would not be. Should the diffusion be very slow, there would be an immediate mass gain of the sample due to surface adsorption. This would be followed by a slow gain as diffusion brings water vapor to the sample interior. The sharp increase in mass, followed by several hours of little or no change could have led to a premature conclusion concerning the attainment of equilibrium.

---

*Model 15-3001 Hygrometer Indicator; Hygrodynamics, Inc; Silver Spring, Md.

experimental results

The results of the present water vapor adsorption study are presented in Figure 7. Superimposed is the isotherm supplied by the manufacturer. While Young's study included silica of 220 m^2/g specific nitrogen BET surface area (Cabot's grade M5 CAB-O-SIL), the data published was for a silica of 420 m^2/g specific area. Comparison is not possible.

Figure 7 shows that the present experimental data match those of the manufacturer up to a relative humidity of about 40%, at which point the present data deviate upward. The situation appears to be that of Young's "initial" and "final" adsorption isotherms. In the present study, no adsorption-desorption hysteresis was observed. At the start of every adsorption trial an initial rapid mass increase was observed. After the first hour or so, mass increases were not perceptible on an hourly basis, but day by day changes did occur. Including the twenty-four hour period of constant mass (the equilibrium attainment constraint) typical trials ran at least two days.

The present work tends to confirm the suspicion concerning previous conclusions about equilibrium attainment. Young's hysteresis anomaly was not observed, but his "initial" - "final" isotherms were valuable clues concerning the speed of approach to equilibrium. In conclusion, the data evolved from the present work, as well as Young's "final" isotherm appear to represent true equilibrium. The experimental isotherm in Figure 7 shall, therefore, be the basis for further study of vapor pressure over mixtures of CAB-O-SIL M5 and sulfuric acid.

FIGURE 7

Equilibrium Water Vapor Adsorption of CAB-O-SIL M5 Silica at 75°F as a Function of Relative Humidity

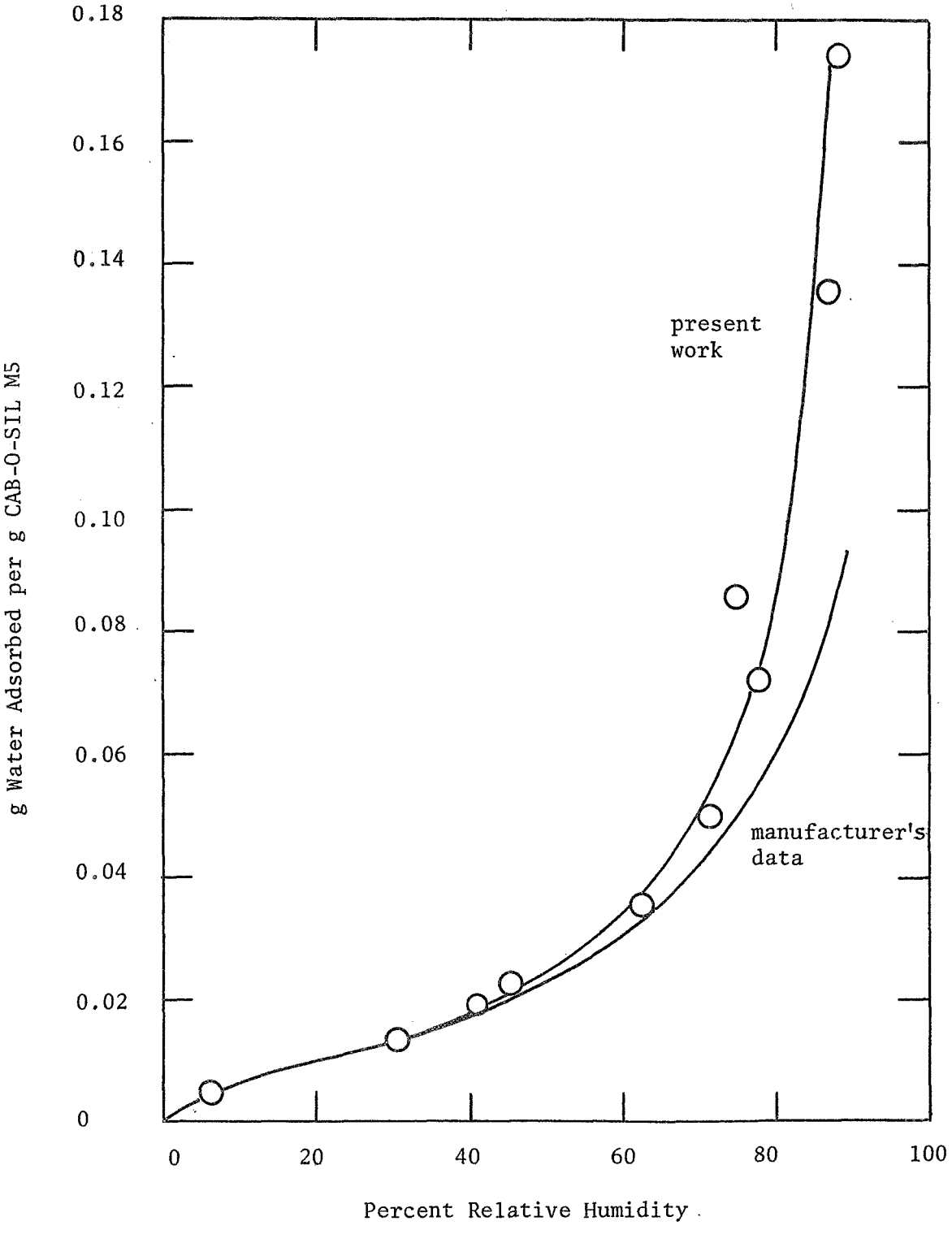

Test of Hypothesis

introduction

Further experimental work was performed on the relative humidity of mixtures of CAB-O-SIL M5 and sulfuric acid. The purpose was an attempt to explain the vapor pressure rise over the mixtures with addition of silica. The hypothesis was that water adsorbed onto the silica before mixing was released upon mixing with acid. The released water caused dilution of the sulfuric acid in the gel, raising the equilibrium relative humidity. The testing of that hypothesis is the subject of this section.

procedure

The method of obtaining data was the same as that described in the Relative Humidity section using the same equipment. In this series, however, the CAB-O-SIL M5 was exposed to environments of different relative humidity. Upon mixing the CAB-O-SIL M5 with sulfuric acid, the equilibrium relative humidity was measured. The apparent new acid strength was calculated from that equilibrium relative humidity and the data in Appendix I. Assuming the amount of H_2SO_4 remained constant, the apparent amount of water in the solution was then calculated. From the mass of water in the acid before the CAB-O-SIL M5 addition, the apparent water gain per unit mass silica added was calculated. The results were then compared with those predicted by the hypothesis.

The expected value of the apparent water gain per unit mass silica was the amount of adsorbed water that the silica contained prior to mixing with the sulfuric acid solution. Agreement between the experimentally determined apparent water gain per unit mass silica added and the expected value would tend to confirm the hypothesis.

results

Experimental data are tabulated in Appendix III for this series of measurements. Two sets of trials have been completed to date. In the first, the CAB-O-SIL M5 was stored in a container open to the atmosphere. During the period of the first set the ambient relative humidity in the laboratory varied from 12 to 19 precent, with an average of 15% RH. The silica thus contained an average of 0.0085 g adsorbed water per g dry silica. Five trials yielded the following result: the average apparent water gain per g silica added was 0.0098 gram. The sample standard deviation was 0.0133 g water added per g silica added, signifying the amount of scatter in the data. A t-test comparing the sample mean and the expected value of 0.0085 yielded a t of 0.219, indicating an 85% probability that the data and the expected value are from the same population. For the second set of trials, the CAB-O-SIL M5 was stored in a dessicator containing a dilute sulfuric acid solution. The relative humidity in the dessicator was measured to be 68.1%. Prior to mixing with the sulfuric acid, the silica contained 0.043 g adsorbed water per g CAB-O-SIL M5. Four trials yielded an average apparent water gain of 0.042 g water per g silica added. The standard deviation was 0.0070 g water per g silica. Comparing the sample mean and the expected value, a t of 0.286 was calculated, corresponding to an 80% probability that the data and the expected value are from the same population. Since an F-test showed the two variances to be similar, they were combined and an average standard deviation of 0.01103 g water per g silica was calculated, with seven degrees of freedom. Comparing the means of the two sample populations, a t of 4.25 was calculated. Since $t_{.99}$ is 3.50 for this case, the two sample populations were highly significantly different.

FIGURE 8

Test of Dilution Hypothesis, Expected Value Versus Measured Sample Means

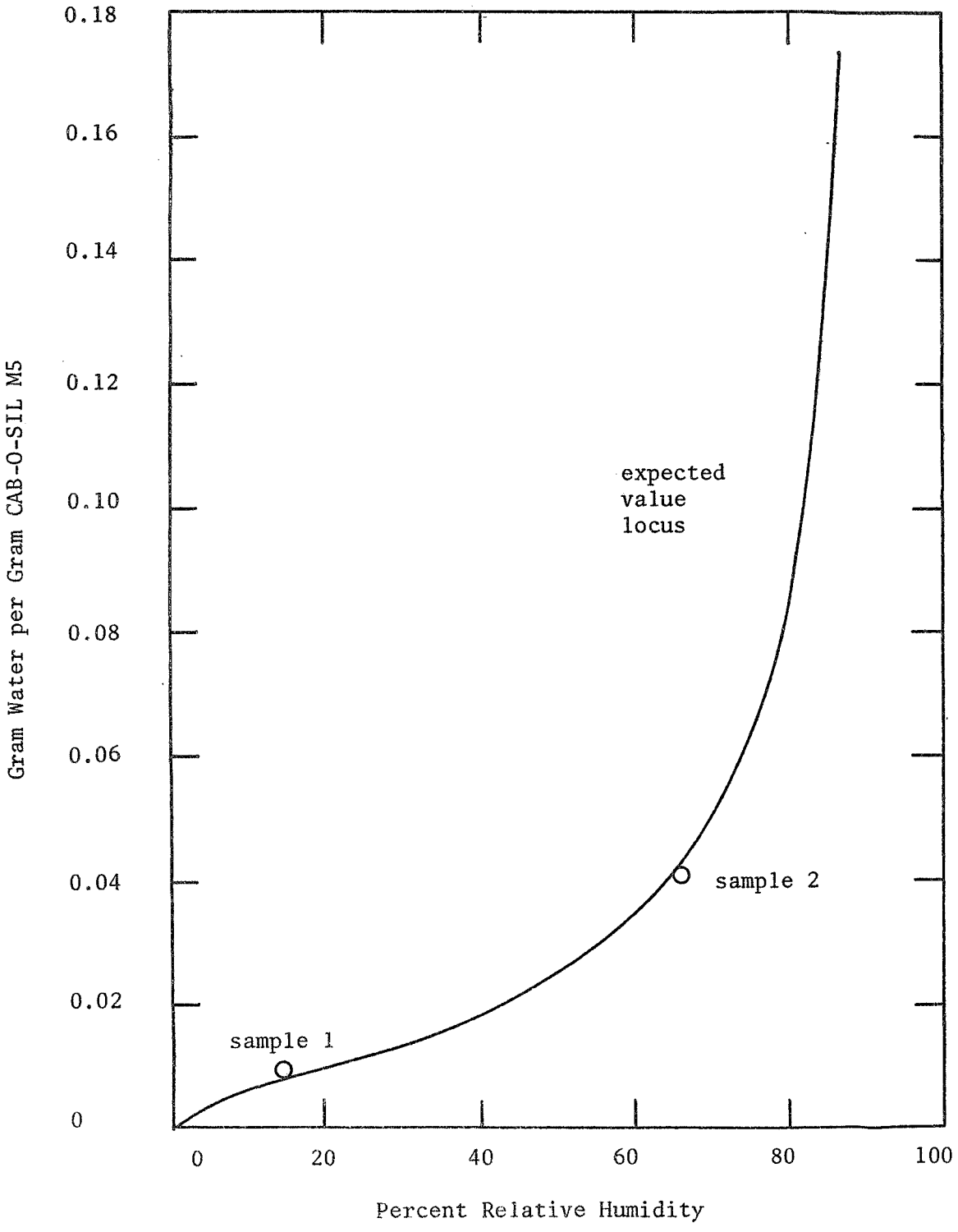

The tests show definitely that relative humidity over the CAB-O-SIL M5 prior to mixing exerts an effect on the equilibrium relative humidity of the CAB-O-SIL M5 - sulfuric acid mixture. There is mild confidence - about 80% - that the hypothesis is valid. There is no validity in discarding the hypothesis.

Figure 8 is the water vapor adsorption isotherm for CAB-O-SIL M5. Superimposed are the means of the two sample populations in the experimental work thus far. The two means being almost coincident with adsorption isotherm show graphically that the hypothesis has merit.

conclusions

Within the limits of experimental work done to date, it appears that CAB-O-SIL M5 has no influence on the relative humidity of mixtures of it and sulfuric acid. Should the CAB-O-SIL M5 have physically adsorbed water on it prior to mixing, however, a dilution of the sulfuric acid will occur upon mixing. CAB-O-SIL M5 dried before mixing of the matrix material exerts no influence on mass transfer. The driving force is dependent on the equilibrium relative humidity of the sulfuric acid alone.

Electrolytic Conductance of Mixtures of CAB-O-SIL M5 and Sulfuric Acid

introduction

In the water vapor electrolysis cell, both mass transfer within the matrix and power consumption are affected by the conductivity of the electrolytic mixture. Previous workers (2, 3, 5, 11), have reported conductivity data. Those reported are for the usual matrix composition of 10 wt% CAB-O-SIL M5 in 60 wt% sulfuric acid. The present work is the first comprehensive study of the effect of CAB-O-SIL M5 on the conductance of sulfuric acid - CAB-O-SIL M5 mixtures.

procedure

The experiment involved measuring the resistivity of known mixtures of sulfuric acid and CAB-O-SIL M5. The acid was approximately 60 wt% H_2SO_4 in water. Mixtures of from zero to ten wt% CAB-O-SIL M5 were studied.

A schematic diagram of the experimental apparatus is shown on Figure 9. The bridge circuit[1] was of the Wheatstone type, excited by a test oscillator[2]. The bridge condition was displayed on a cathode ray tube (CRT) oscilloscope. Balance for an impedance bridge is defined by the voltages at the opposite arms (points A and B in Figure 9) being of equal magnitude and phase. Phase was equalized by adjusting the frequency of the test oscillator output. Magnitude was equalized by adjusting the resistors in the bridge circuit.

The voltages at points A and B in Figure 9 drive the horizontal and vertical oscilloscope inputs respectively. At bridge balance, the CRT display is a straight line of 45° slope, symmetric about the axes. When the voltages at points A and B are out of phase, the CRT display is an ellipse, whose quadrant II-IV axis is proportional to the phase shift. When the voltages at points A and B are of different magnitude, the quadrant I-III axis inclination differs from 45°.

The conductivity cell (impedence Z_c in Figure 9) was of the standard dip type, with firmly anchored platinum electrodes. Dipping the cell into mixtures of CAB-O-SIL M5 and sulfuric acid was possible up to about 6 wt% CAB-O-SIL M5. At higher concentrations of silica, the gel

---

[1]Model E1000, Gray Instrument Co, Philadelphia, Pa.

[2]Model 650A, Hewlett Packard Co, Palo Alto, California

FIGURE 9

Experimental Apparatus for the Measurement of Electrolytic Resistivity of Mixtures of 60 wt% Sulfuric Acid and CAB-O-SIL M5 Silica, Showing the Measuring Circuit Diagram and the CRT Oscilloscope Display of the Voltages at Points A and B of the Bridge Circuit

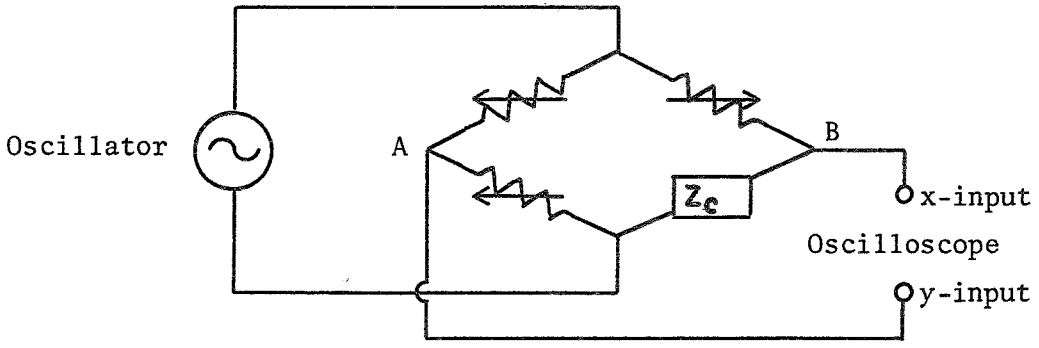

Schematic Diagram of Circuit

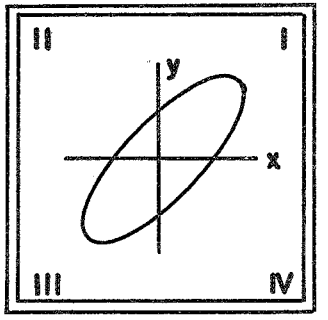

CRT Display

was too thick for dipping. Thus, the semisolid was spooned into the dip cell and forced between the plates by spreading with a spatula. Spreading was continued until no further change in resistance was observed, indicating the complete covering of the electrodes.

Several sulfuric acid strengths between 55 and 65 wt% were tested. In view of the possibility of altering the configuration of the electrodes - especially with the semisolid mixtures - a reference measurement (aqueous sulfuric acid alone) was made before each data set was gathered. Rather than continuously measuring the cell constant, the data were gathered and are reported in dimensionless form. That form is the change in resistance from the reference divided by the reference - $\Delta R/R_o=(R_f-R_o)/R_o$.

Since the measured resistance of impedence Z_c is the product of the cell constant and the resistance of the electrolyte, the dimensionless resistance change is equal to the dimensionless resistivity change.

results

The experimental results are displayed graphically in Figure 10, showing the dimensionless resistivity change as a function of wt% CAB-O-SIL M5 in sulfuric acid.

Within the range of acid strengths studied, the dimensionless resistance change was not a function of acid strength, indicating dependence on wt% CAB-O-SIL M5 only. Figure 10 shows the change of resistance from aqueous sulfuric acid alone to be a linear function of wt% CAB-O-SIL M5 in the mixture. Linear regression gives a least squares fit of the data to the following equation:

$$\Delta R/R_o = (0.0240) * (\text{wt\% CAB-O-SIL M5})$$

FIGURE 10

Dimensionless Resistivity Change of Mixtures of 60 wt% Sulfuric Acid and CAB-O-SIL M5 Silica as a Function of wt% Silica in the Mixture

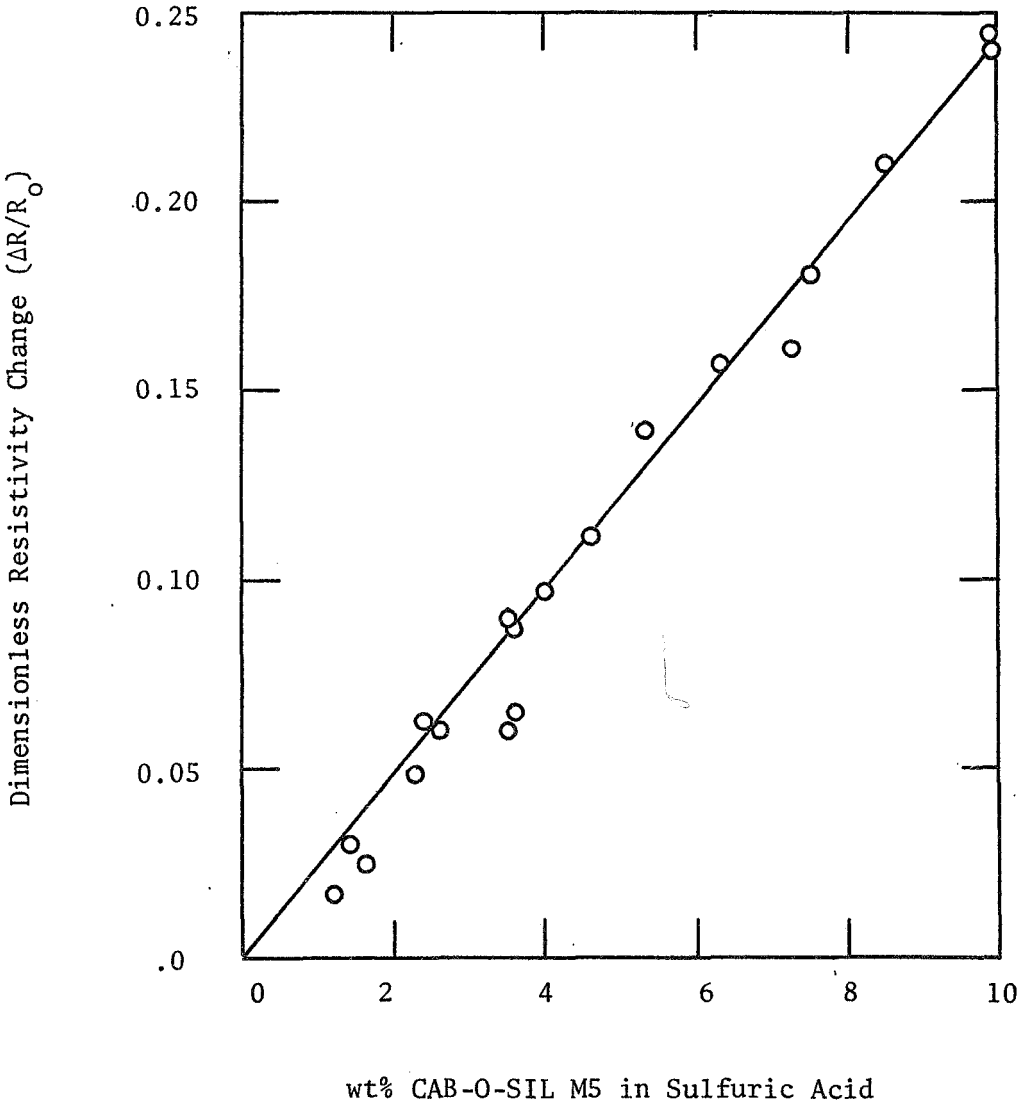

CYCLIC OPERATION OF THE WATER VAPOR ELECTROLYSIS CELL

Introduction

In a preliminary investigation, Engel (7) discovered that cycling of the power supply to the cell resulted in improved performance. That is, the power required to electrolyze a given amount of water could be reduced by varying the applied cell voltage. It was the purpose of the present work to optimize the cell's power consumption as a function of cyclic operation, building on the work of Engel.

Engel reported that "on/off" cycling was the only type capable of effecting the performance increase. After a given time under power, the power was disconnected and both electrodes of the cell grounded. Simultaneous grounding of the PVC central membrane was found to decrease the time required for the capacitative discharge to ground. The cycling was shown to decrease by as much as eight percent the power required to electrolyze a given amount of water. Engel's hypothesis to explain the performance increase was the following:

> "...any improvements due to cycling are caused by some type of regeneration of one or both of the electrodes to make them more active."

The "regeneration" referred to the effect of time of steady state operation prior to cycling in performance increase. The cycling had a greater influence on performance with longer prior steady state time.

The present work is intended to experimentally determine the optimum cycle as well as the optimum steady state/cycling combination.

Experimental Work

Cyclic operation of the water vapor electrolysis cell was affected by the electric circuit diagrammed in Figure 11.

The cyclic operation of this circuit in Figure 11 was controlled by two timers, A and B. They were loaded with the selected "on" time (Timer A) and the "off" time (Timer B), for a cycle. When one timer counted down to zero, it would reset and start the other timer. The circuit diagram shows logical control of the two relays. The state of the timer is either "true/on" or "false/off". If the state of timer A is "true", the flip-flop sets and puts the relays in their "true" positions. When the state of Timer B is true, the flip-flop resets, putting the relays in their "false" positions.

The logic control in the diagram is, for simplification, an abstraction of the electro-mechanical system used.

The other circuit components shown in Figure II are the electrolysis cell, a variable dc power source, and a resistance R1. The DC power source[1] was capable of operating in either constant current or constant voltage mode. The resistance R1 was an NBS type 0.1 ohm precision resistor[2] and was used to measure the current drawn by the cell.

Since the performance was measured by the amount of power required to electrolyze a given amount of water in the test cell, a suitable integrating recording wattmeter was required. Such was not commercially available. A small electronic analog computer was constructed to perform the task. The voltage drop across the test cell and the voltage

---

[1]Model CK5-M, Kepco, Flushing, N. Y.

[2]Model 4015-B, Leeds and Northrup, North Wales, Pa.

FIGURE 11

Schematic Diagram of the Circuit for the Cyclic Operation of the Water Vapor Electrolysis Cell

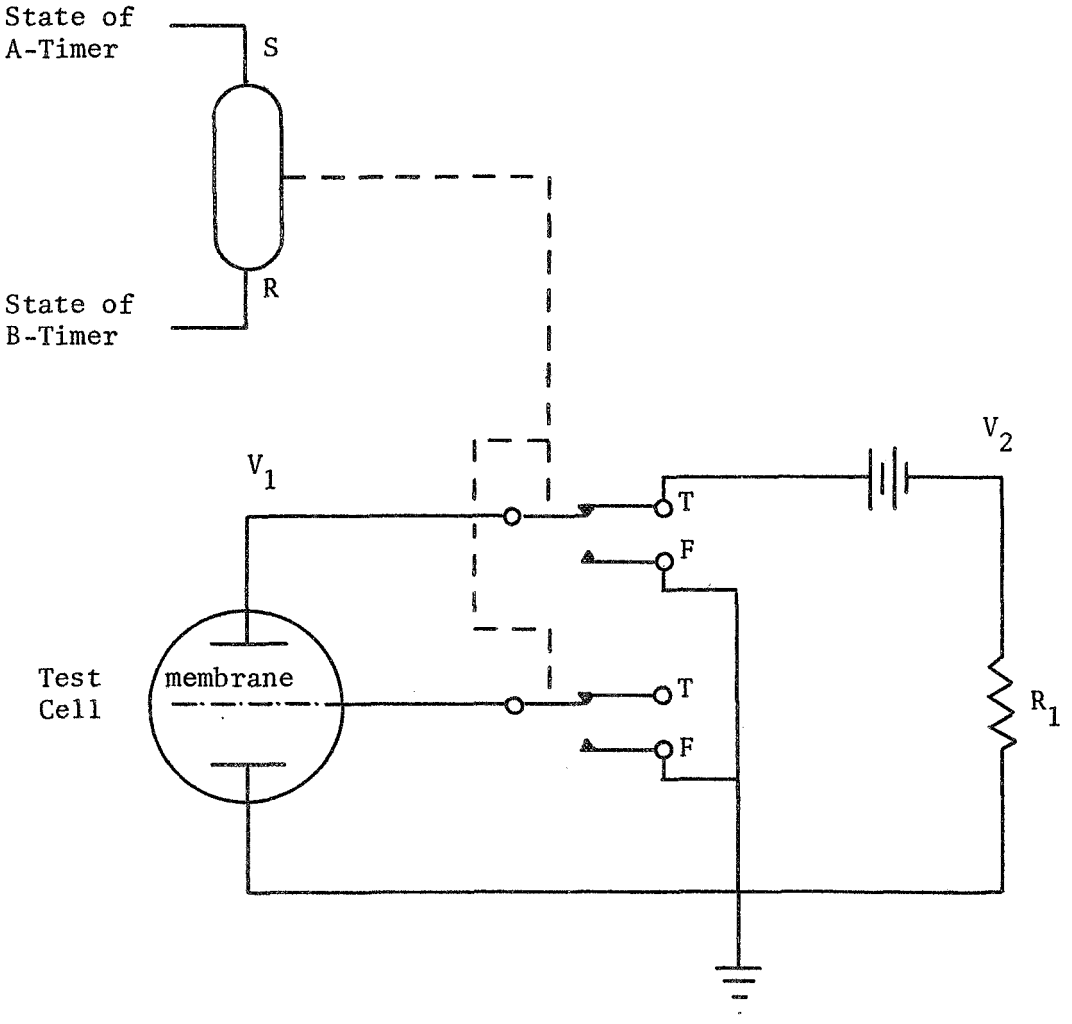

drop across the precision resistor (proportional to the current drawn) were multiplied and integrated with respect to time. Instantaneous and integral power were displayed on a two-channel strip chart recorder. Figure 12 is a schematic diagram of the computer.

In Figure 12 the potentiometers A, B and C are used to attenuate voltage as desired to fit the range of the recorder and the linear range of the integrator. Since V_1 is one tenth the current drawn, the voltage leaving the multiplier is (AB/50) times the instantaneous power, and the integration output is (ABC/250) times the integral of that power with respect to time. The "gain" of the integrator, ABC/250, is to be trimmed such that its output does approach but does not exceed the 5-volt limit of the element during the time period of interest.

The time period of interest for this study is the amount of time required to electrolyze a given amount of water. Hydrogen evolution at the cathode was chosen as a convenient measure of the electrolysis cell's production. The gas passed through a soap bubble flow-meter, and an electric timer measured the amount of time required for a specific volume to be evolved.

Electrolysis cell operation required, beyond the preceding electrical circuitry, a known supply of humid air for operation. The air supply system used in the present work has been assembled. Constant-pressure air enters the system and flows toward a humidifying chamber. Part of the air stream is bubbled through warm water for humidification and part passes through a coil immersed in the water. The two streams rejoin each other upon leaving the water bath. Air temperature is controlled by regulating the temperature of the water bath. Air humidity is varied by changing the proportion of the air stream flowing through the bubbler.

FIGURE 12

Schematic Diagram of the Special Purpose Analog Computer Used As An Indicating/Integrating Wattmeter

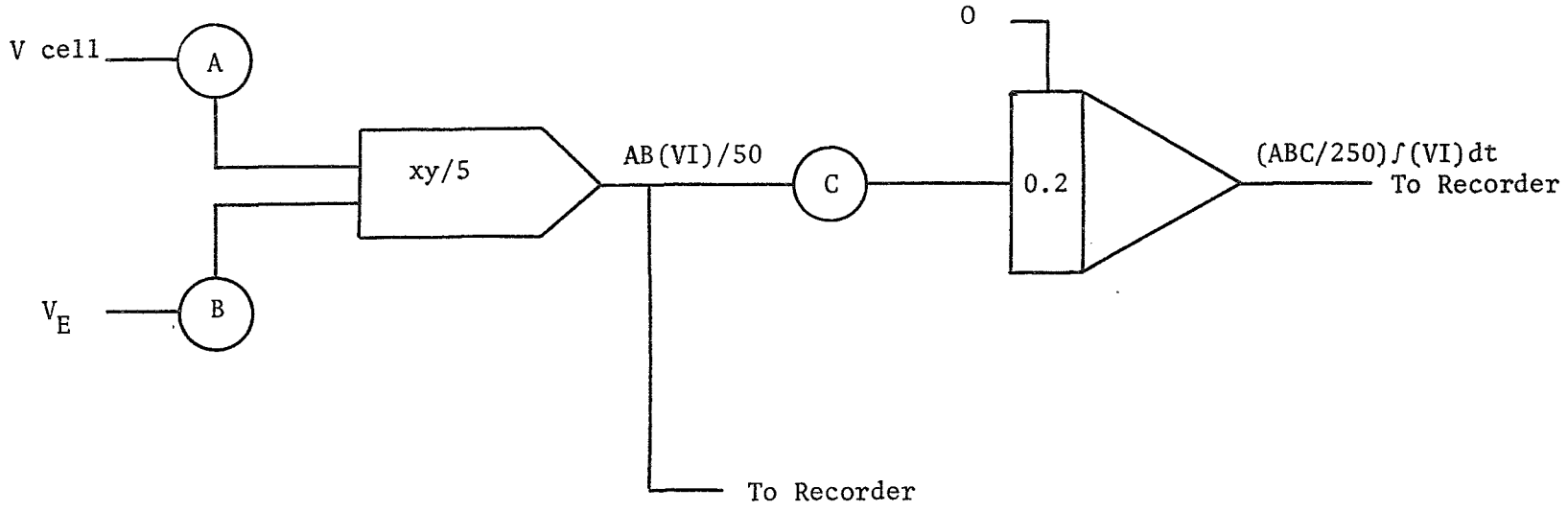

The air stream then flows through a rotameter and a chamber containing a temperature-humidity sensor. The stream then passes through the electrolysis cell and is vented. When the temperature and humidity of the exit air stream are to be measured, a rather complicated system of valves changes the flow pattern such that the cell's inlet air stream bypasses the T-H sensor chamber and the exit air stream enters the chamber.

results

There are no experimental results to date. Fabricators and suppliers held up even the assembly of experimental apparatus until October 1969. The hygrosensing apparatus was and is being used on the physical-chemical experimental work. With no funds, duplicate equipment is out of the question. It is predicted that the experimental work on this segment will begin no later than 1 April 1970.

LIST OF REFERENCES

1. Bird, R. B., et. al., "Transport Phenomena", John Wiley and Sons, Inc., New York (1959).

2. Clifford, J. E., "Water Vapor Electrolysis Cell with Phosphoric Acid Electrolyte", paper presented at SAE Aeronautic and Space Engineering and Manufacturing Meeting, Los Angeles, Calif., (October 1967)

3. Clifford, J. E., et. al., Batelle Memorial Institute, NASA Contract No. NAS 2-2156, Final Report, (February 1969).

4. Cochrane, H., Cabot Corp., Billerica Research Center, communication, (3 November 1969).

5. Connor, W. J., et. al., Lockheed Missiles and Space Company, NASA Contract No. NAS 2-2630, Final Report, (March 1966).

6. Eitel, W., "Silicate Science, Vol. 1", Academic Press, New York, (1964).

7. Engel, A. J., ASEE-NASA Summer Institute, Final Report, (1967).

8. Engel, A. J., ASEE-NASA Summer Institute, Final Report, (1968).

9. Schlichting, H., "Boundary Layer Theory", McGraw Hill, New York, (1960).

10. Stokes, R. H. and R. A. Robinson, Industrial and Engineering Chemistry, 9, 2013, (1949).

11. Wydevan, T. and E. Smith, Aerospace Medicine, 1045, (October 1967).

12. Young, G. J., Journal of Colloid Science, 13, 67, (1958).

APPENDIX I. RELATIVE VAPOR PRESSURE OF H_2SO_4 SOLUTIONS

The physical-chemical studies of the sulfuric acid and CAB-O-SIL M5 system required accurate data on the water activity of solutions of sulfuric acid. The data of Stokes and Robinson (10) were selected as the best available. Their data, tabulating water activity as a function of sulfuric acid concentrations at 25 degrees Celsius, are presented in Table I-1 below.

Table I-1

Equilibrium Activity of Water of Solutions of Sulfuric Acid at 25°C

a_W	wt% H_2SO_4	a_W	wt% H_2SO_4
.90	17.91	.45	45.41
.85	22.88	.40	47.71
.80	26.79	.35	50.04
.75	30.14	.30	52.45
.70	33.09	.25	55.01
.65	35.80	.20	57.76
.60	38.35	.15	60.80
.55	40.75	.10	64.45
.50	43.10	.05	69.44

Since the above data are for 25 degree Celsius, a correction factor for deviations from that temperature is required. Vapor pressure-concentration data for aqueous sulfuric acid are presented in the International Critical Tables at various temperatures. Though the data are not self-consistent, a sufficient number taken together offer some validity. In the region of interest - 50 to 65 weight percent acid and 20 to 30 degree Celsius - a useful correction

factor was found, an average of

$$\frac{d\ RH}{dt} = 0.034\ \%RH\ /\ °F$$

The t-distribution yielded the information that the true value could be expected to be within $\pm$ 0.007 %RH/°F of the above average with 0.95 confidence. Percent relative humidity measurements with the T-H indicator yield significant figures only to the first decimal place. The correction factor could thus confidently be expected to account for small temperature effects on humidity measurements.

APPENDIX II. ADSORPTION DATA

In this section, data concerning the study of equilibirum water vapor adsorption by CAB-O-SIL M5 are presented. The data here are in tabular form and are more complete than those presented in the main body of the paper.

Manufacturer's Data

First, the data supplied by the manufacturer are listed. Table II-1 below shows the data points for the supplied equilibrium isotherm at 75% F.

TABLE II-1

Water Vapor Adsorption Isotherm for CAB-O-SIL M5 at 75°F, Data Supplied by Cabot Corporation, Billerica Research Center.

% RH	gH_2O adsorbed/ g adsorbent
6.9	.00504
19.5	.00905
32.35	.0161
44.75	.0217
54.1	.0265
64.2	.0360
80.5	.0618
86.8	.0910
89.5	.1155

PRESENT WORK

Secondly, data gathered in the present experimental study are presented. Since the adsorption isotherm was determined gravimetrically, the quartz spring used had to be calibrated. Then raw adsorption data were taken, and the data converted to g water adsorbed per g adsorbent. Each of these is discussed in turn.

Spring Calibration

The quartz spring used was rated for a maximum spring extension of 20 centimeter under a maximum load of two grams. Four masses of approximately 0.5, 1.0, 1.5, and 2.0 gram were constructed for purposes of calibration of load versus extension. The masses were accurately weighed on a Metlar type analytical balance to 0. 1 mg. Those masses were determined to be the following:

mass no.	mass
1	0.5350 g
2	1.1295 g
3	1.6039 g
4	1.8658 g

These loads were then suspended from the spring, and the spring's extension noted. The results were:

mass no.	spring extension trial 1	trial 2	trial 3	spring coefficient
1	5.34 cm	5.34 cm	5.34 cm	0.10019 g/cm
2	11.28	11.30	11.29	0.10004
3	15.99	15.99	15.99	0.10031
4	18.58	18.61	18.59	0.10037

Three trials were all that were necessary to be confident that a value of the spring coefficient of 0.100 gram per centimeter extension was valid over the range investigated.

Adsorption Data

The first series began with 500 ml of concentrated sulfuric acid in the humidity chamber to dry the sample. It was diluted with 500 ml of water upon reaching equilibrium. The trial was halted at this point, as circulated air caused acid spray to come close to the lithium hydroxide-covered sensing element. The data are the following:

trial	relative humidity	spring elevation	comments
		94.11 cm	empty sample bucket
1	0 %	90.10 cm	0.401 g dry silica
2	6.35 %	90.08 cm	0.002 g water gained

The second series was a desorption trial, beginning with 500 ml water in the humidity chamber, then adding sulfuric acid to decrease the relative humidity. The data are tabulated below:

trial	relative humidity	spring elevation	comments
	*******	93.86 cm	empty sample bucket
1	100 %	******	water condensate
2	88.1 %	90.82 cm	0.045 g water gained
3	71.3 %	91.14 cm	0.013 g water gained
4	41.0 %	91.22 cm	0.005 g water gained
5	0	91.27 cm	0.259 g dry silica

Apparent small temperature differences between the two chambers caused water condensation in the adsorption chamber during the 100%RH run. In the above table, water weight gain was back calculated from trial 5.

Summarizing the results of series one and two,

relative humidity	g water adsorbed per g CAB-O-SIL
6.35 %	0.005
41.0 %	0.0193
71.3 %	0.0502
88.1 %	0.174

The third series was another adsorption run. The results are summarized below:

trial	relative humidity	spring elevation	comments
	******	94.60 cm	empty sample bucket
1	0	93.4925 cm	0.11075 g dry silica
2	30.5 %	93.4775 cm	0.0015 g water gained
3	45.2 %	93.4675 cm	0.025 g water gained
4	62.4 %	93.4530 cm	0.00395 g water gained
5	77.1 %	93.4125 cm	0.00800 g water gained
6	86.7 %	93.3425 cm	0.01500 g water gained
7	74.8 %	93.3975 cm	0.00950 g water gained

Converting and summarizing the results of the three adsorption experiments, the adsorption isotherm is presented in Table II-2.

Table II-2

Water Vapor Adsorption Isotherm for CAB-O-SIL M5 at 75° F,

Experimental Data, Present Work

relative humidity	g water adsorbed per g adsorbent
6.35 %	0.0050
30.50 %	0.0135
40.30 %	0.0193
45.20 %	0.0226
62.40 %	0.0357
71.20 %	0.0501
74.80 %	0.0858
77.10 %	0.0722
86.70 %	0.1354
88.10 %	0.1730

APPENDIX III. EXPERIMENTAL DATA FOR THE EQUILIBRIUM RELATIVE HUMIDITY OF MIXTURES OF SULFURIC ACID AND CAB-O-SIL M5 SILICA

The data listed in Table III-I were gathered to further investigate the rise in equilibrium relative humidity with wt% CAB-O-SIL M5 in sulfuric acid. The hypothesis advanced was that the silica had adsorbed atmospheric water vapor in storage and had released it upon mixing with this acid, causing a dilution of the bulk sulfuric acid. The dilution was the reason for an increased equilibrium relative humidity. The data in Table III-I was taken to test the hypothesis.

The table is divided into three sections. A trial started with a known mass of aqueous sulfuric acid of known composition. For these data are calculated the amount of H_2O and H_2SO_4 present in the system at the beginning of the trial. Then a known mass of CAB-O-SIL M5 silica was added.

The atmospheric relative humidity in contact with the silica before mixing was noted. When the silica-sulfuric acid mixture came to equilibrium, its relative humidity was measured. From this, the apparent sulfuric acid strength was calculated. Assuming a constant mass of H_2SO_4, an apparent new mass of H_2O was calculated. The apparent H_2O gain of the acid per unit mass silica added was then calculated. This last value was to be compared with the mass of adsorbed water contained by the silica before mixing - known from the % RH over the stored CAB-O-SIL M5 and the water vapor adsorption isotherm.

TABLE III-1. EXPERIMENTAL EQUILIBRIUM % RH DATA FOR MIXTURES OF CAB-O-SIL M5 AND SULFURIC ACID.

Before Silica Addition				mass CAB-O-SIL added, g	% RH over stored silica	At Equilibrium			
mass aqueous sulfuric acid, g	wt% H_2SO_4	mass H_2SO_4, g	mass water, g			% RH over silica-acid mixture	Apparent wt% acid	Apparent water gain, g	g water gain per g silica added
205.55	59.68	122.66	82.89	8.50	16	16.90	59.65	0.15	0.018
204.06	59.65	121.77	82.29	12.93	12	16.83	59.69	0.10	0.008
103.79	59.68	61.94	41.85	3.45	17	17.14	59.62	0.08	0.024
141.74	59.68	84.58	57.16	10.06	19	16.90	59.65	0.10	0.010
102.16	59.68	60.96	41.20	10.43	13	16.80	59.70	0.11	0.011
30.79	57.71	18.38	12.41	3.01	68	17.19	59.47	0.11	0.038
252.14	58.19	146.72	105.42	5.26	68	19.35	58.15	0.17	0.033
252.02	58.15	146.55	105.47	8.33	68	19.51	58.06	0.38	0.048
249.55	58.06	144.89	104.66	5.66	68	19.67	57.96	0.25	0.046

APPENDIX IV. ELECTROLYTIC CONDUCTANCE DATA, MIXTURES OF CAB-O-SIL M5 AND SULFURIC ACID, AT 75°F.

TRIAL	MASS H_2SO_4	MASS CAB-O-SIL M5	WT% CAB-O-SIL M5	R	ΔR/R
1	255.40 g	0	0	3.3	0
1a		3.715 g	1.4	3.4	0.03
1b		6.765 g	2.6	3.5	0.06
1c		9.185 g	3.5	3.5	0.06
1d		9.320 g	3.5	3.6	0.09
2	302.045 g	0	0	2.85	0
2a		3.655 g	1.2	2.90	0.017
2b		7.385 g	2.4	3.03	0.063
2c		11.095 g	3.6	3.10	0.087
2d		13.905 g	4.6	3.17	0.112
2e		16.015 g	5.3	3.25	0.140
2f		19.185 g	6.3	3.30	0.157
3	204.515 g	0	0	2.85	0
3a		20.395 g	9.9	3.55	0.245
4	204.515 g	0	0	2.24	0
4a		20.395 g	9.9	2.78	0.241
5	117.700 g	0	0	2.85	0
5a		10.94 g	8.5	3.45	0.211
6	216.21 g	0	0	2.45	0
6a		3.58 g	1.6	2.51	0.025
6b		7.96 g	3.6	2.61	0.065
7	253.41 g	0	0	3.10	0

APPENDIX IV (continued).

TRIAL	MASS H_2SO_4	MASS CAB-O-SIL M5	WT% CAB-O-SIL M5	R	ΔR/R
7a		5.885 g	2.30	3.25	0.049
7b		10.615 g	4.00	3.40	0.097
7c		19.795 g	7.24	3.60	0.161
8	69.1	0	0	3.05	0
8a		5.575 g	7.5	3.60	0.181

and advanced undergraduates of many disciplines and representatives of air pollution control agencies at the local, state, and federal level.

The Air Pollution Specialist Training Program is an intensive course designed to provide specialized knowledge and skills necessary for work in air pollution control instrumentation for field monitoring and sampling. The program involves one term of full time work on campus for students who have completed at least one year in their studies for an associate degree in engineering technology. Also initiated under this program is a Pennsylvania survey of vegetation damage. Agricultural extension personnel and county agents were trained to recognize air pollution damage to crops and are now reporting damage seen in their daily work to the Center for analysis.

Address requests for more information concerning the training programs to the Director, Center for Air Environment Studies, The Pennsylvania State University, University Park, Pennsylvania 16802.

Publications Available

AIR POLLUTION TITLES, a current awareness publication service, is available on a January-December subscription basis. This publication is a quick guide to current literature and has some capacity as a retrospective searching tool. APT uses a computer-produced, Keyword-in-Context (KWIC) format to provide a survey of current air pollution and related literature. During the year over 1,000 journals are scanned for pertinent citations.

Subscriptions to APT at $15/year, cover six issues per year as follows: No. 1, January-February; No. 2, March-April; No. 3, May-June; No. 4, July-August; No. 5, September-October; No. 6, cumulative issue for the year, including November-December citations. The 1970 subscription of APT is now available. Complete subscriptions for 1967, 1968, and 1969 are out of supply. However, cumulative issues for 1967, 1968, and 1969 are being issued; the cost is $10 each.

INDEX TO AIR POLLUTION RESEARCH was published in July of 1966, 1967, and 1968. Each Index included government sponsored research in the air pollution field and the results of a survey of air pollution research projects conducted by the industrial, sustaining, and corporate members of the Air Pollution Control Association and the American Industrial Hygiene Association, and research supported by other industries and non-profit organizations.

The Index utilizes the Keyword-in-Context (KWIC) format for rapid scanning of project titles. In addition, this publication provides a complete bibliography including mailing addresses where additional information about the project may be obtained. Beginning with the 1967 edition, a section containing citations of papers resulting from the research in progress was included. Copies of the 1966 and 1967 editions are available at $1.25 each. The 1968 edition costs $2.

HANDBOOK OF EFFECTS ASSESSMENT VEGETATION DAMAGE was published in 1969 as part of the survey of vegetation damage. It describes in detail the many sources of pollution and the effect on vegetation and includes color pictures showing characteristics of plant damage symptoms. The cost is $6 each.

Requests for additional information and orders should be addressed to: Information Services, Center for Air Environment Studies, University Park, Pennsylvania 16802.

NOTE: The National Air Pollution Control Administration of the United States Public Health Service selected the Center for Air Environment Studies to prepare A Guide to Air Pollution Research which paralleled and replaced the 1969 Index. By contract agreement, the National Administration is managing the distribution of all copies.